

AD618368

Permission to release to  
Clearinghouse for Federal Scientific  
and Technical Information given by  
U S Naval Ordnance Test Station,  
China Lake

NAVWEPS REPORT 8505  
NOTS TP 3487  
COPY 92

# MEASUREMENT OF PARTICLE VELOCITIES IN SUPERSONIC GAS STREAMS

by

Richard D. Fulmer and David P. Wirtz  
Propulsion Development Department

DDC  
AUG 2 1965  
DDC-IRA E

COPY	OF	30
HARD COPY	\$.	3.00
MICROFICHE	\$.	0.50

52-P

**ABSTRACT.** A photographic technique was developed at the U. S. Naval Ordnance Test Station, China Lake, to directly measure the velocity of particles as small as 2-3 $\mu$ -diameter traveling at velocities up to 2,600 ft/sec in supersonic gas streams. A double-pulsed explosive-krypton light source was used to provide intense and precisely controlled light pulses that were used both for illuminating and shuttering the event. The particle images were recorded on film as pairs of streaks. The velocities of the particles were determined from the magnification of the camera-lens system, the measured distance between the streaks on the film, and the time interval between flashes.

A series of ten runs was made in which the velocity of 3-50 $\mu$  particles were measured as they were carried in a 2,900 ft/sec helium stream. Particle velocities up to 2,600 ft/sec were measured with an accuracy of from 1.5 to 3.2%. By optimizing the technique it should be possible to extend the measurements to higher particle velocities. Particle velocities and sizes were correlated and the results compared with theoretical data calculated using a one-dimensional treatment with constant lag assumptions. Although the data trends correlate well, it appears that particle lag is not as great as predicted by theory.



U. S. NAVAL ORDNANCE TEST STATION

China Lake, California

December 1964

ARCHIVE COPY

**U. S. NAVAL ORDNANCE TEST STATION**

AN ACTIVITY OF THE BUREAU OF NAVAL WEAPONS

**J. I. HARDY, CAPT., USN**  
*Commander*

**WM. B. McLEAN, PH.D.**  
*Technical Director*

FOREWORD

The work described in this report was supported by Exploratory and Foundational Research funds, WepTask R360-FR 106/216-1/ROLL-01 01, and was performed during Fiscal Year 1963.

The report was reviewed for technical accuracy by Dr. H. D. Mallory of the Propulsion Development Department and Mr. W. H. Allan of the Weapons Development Department, and is transmitted for information purposes only.

Released by  
R. T. MERROW, Acting Head,  
Advanced Technology Division  
22 December 1964

Under authority of  
G. W. LEONARD, Head,  
Propulsion Development Dept.

NOTS Technical Publication 3487  
NAVWEPS Report 8505

Published by ..... Propulsion Development Department  
Collation ..... Cover, 26 leaves, abstract cards  
First printing ..... 205 numbered copies  
Security classification ..... UNCLASSIFIED

**BLANK PAGE**

CONTENTS

Introduction .....	1
Measurement Technique Development .....	1
Camera and Film Unit .....	2
Illumination .....	4
Flow Apparatus .....	9
Particles .....	11
Integrated Setup .....	12
Pretest Alignment .....	13
Firing Sequence .....	13
Particle Velocity Measurements .....	13
Experimental Equipment .....	15
Flow Field Studies .....	15
Particle Problems .....	15
Experimental Arrangement and Procedures .....	16
Results and Discussion .....	16
Conclusions .....	30
Appendixes: .....	
A. Survey of Photographic Methods for the Direct Measurement of Particle Velocities .....	31
B. Explosive Rare-Gas Light Bomb .....	40
References .....	46

---

Figures:

1. Explosive Rare-Gas Light Bomb .....	6
2. Exploded View of the Inner System and Focusing Lens of the Explosive Rare-Gas Light Bomb .....	7
3. Streak Camera Record Showing Light Output Pattern for Explosive Rare-Gas Light Bomb Arranged for Dual Pulse Operation .....	9
4. Alignment of Nozzle, Light Bomb and Camera .....	10
5. Particle Generator .....	11

6.	Test Arrangement for Particle Velocity Tests .....	12
7.	Particle Measurement Test Setup .....	14
8.	Photomicrograph of the Particles in Fraction 1 (200X Magnification) .....	17
9.	Photomicrograph of the Particles in Fraction 2 (200X Magnification) .....	17
10.	Photomicrograph of the Particles in Fraction 3 (200X Magnification) .....	18
11.	Photomicrograph of the Particles in Fraction 4 (200X Magnification) .....	18
12.	Size Distribution for Aluminum Powder Fractions Used in Particle Velocity Measurements .....	19
13.	Streak Photographs of Small Particles in a 2,900 ft/sec Helium Gas Stream. Particle Fraction 1. Run D1 .....	21
14.	Streak Photographs of Small Particles in a 2,900 ft/sec Helium Gas Stream. Particle Fraction 1. Run D2 .....	21
15.	Streak Photographs of Small Particles in a 2,900 ft/sec Helium Gas Stream. Particle Fraction 1. Run D3 .....	22
16.	Streak Photographs of Small Particles in a 2,900 ft/sec Helium Gas Stream. Particle Fraction 1. Run D4 .....	22
17.	Streak Photographs of Small Particles in a 2,900 ft/sec Helium Gas Stream. Particle Fraction 2. Run D5 .....	23
18.	Streak Photographs of Small Particles in a 2,900 ft/sec Helium Gas Stream. Particle Fraction 2. Run D6 .....	23
19.	Streak Photographs of Small Particles in a 2,900 ft/sec Helium Gas Stream. Particle Fraction 3. Run D7 .....	24
20.	Streak Photographs of Small Particles in a 2,900 ft/sec Helium Gas Stream. Particle Fraction 3. Run D8 .....	24
21.	Streak Photographs of Small Particles in a 2,900 ft/sec Helium Gas Stream. Particle Fraction 4. Run D9 .....	25
22.	Streak Photographs of Small Particles in a 2,900 ft/sec Helium Gas Stream. Particle Fraction 4. Run D10 .....	25

23.	Particle Velocity Distribution for the Various Aluminum Powder Fractions (2,900 ft/sec Helium Carrier Gas) .....	28
24.	Normalized Particle Velocity as a Function of Particle Size Using a Helium Carrier Gas Moving at 2,900 ft/sec .....	29
25.	Schematic Drawing of Multiple Image Backlighting Setup .....	33
26.	Idealized Pictures Obtained With Multiple Image Backlighting Technique (Fig. 25) .....	33
27.	Idealized Picture From Single Streak Technique .....	34
28.	Idealized Picture From Multiple Streak Technique Frontlighted .....	36
29.	Schematic Diagram of Streak Camera Setup for Photographing Particle Flows .....	37
30.	Idealized Picture Obtained With Streak Camera Technique ....	38
31.	Light-Bomb Housing .....	41
32.	Assembled Inner Light Bomb System .....	42
33.	Dual Streak Light Pulse Pattern .....	43
34.	Light Condensing Lens System .....	45

#### ACKNOWLEDGEMENT

The authors are indebted to Dr. Clayton T. Crowe of the United Technology Center for his assistance in the determination of theoretical particle lag data. Special acknowledgement is also due Wallace H. Allan of the U. S. Naval Ordnance Test Station for his consultation in the area of photographic techniques and light sources.

## INTRODUCTION

Investigators in the past were puzzled by the fact that a number of high-energy propellants containing metal additives were not producing the specific impulses predicted by theory. A closer examination of the problem revealed that one of the causes of degradation was the relatively large amount of solid and liquid particles in the exhaust stream. These condensed-combustion products lag the gas stream in velocity and must be accelerated by dissipative drag forces. In addition, the particles cannot transfer their heat fast enough to maintain temperature equilibrium with the gas as it expands and cools in the nozzle. As a result, the particles usually leave the motor at higher temperatures than the gas and, in the process, carry off thermal energy that otherwise could have been converted into kinetic energy. The end result of the two loss mechanisms is a lower exhaust velocity and degradation of motor performance. In order to better predict these losses and to aid in the analysis of gas-particle systems, an accurate theory is needed to account for the effects of multiphase flow.

The characteristics of gas-particle flows have been widely investigated. Most of the work was carried out on a theoretical level and various models were proposed to predict the fluid dynamics of such systems (Ref. 1-2). Most of the experimental work to date has consisted of inferring the effects resulting from the presence of the particles by using the measured motor parameters such as thrust, specific impulse, etc. Experimental information, however, is needed concerning the behavior of individual particles to verify the theoretical models and to supply input data needed in the theoretical calculations.

This report describes an experimental program conducted at the Naval Ordnance Test Station during FY 1963 from which a technique was developed to directly measure the velocities of small, individual particles traveling in high-velocity gas streams. The report is divided into two principal sections: (1) development of particle velocity measurement techniques, and (2) measurement of particle velocities.

## MEASUREMENT TECHNIQUE DEVELOPMENT

A study was conducted on the state-of-the-art photographic techniques applicable to the measurement of particle velocities (Appendix A). As a result of the study a promising technique was chosen because it was relatively simple and inexpensive.

The technique incorporates an explosive rare-gas light bomb and a simple press-type camera to obtain pictures of the particles and the measurements of their velocities. The light bomb was constructed in such a way that two extremely intense and precisely timed light pulses were produced. These pulses were used to directly illuminate the



particles and to shutter the event. The camera shutter remained open during the entire event and the particle images were recorded as pairs of streaks on the film. By knowing the magnification of the camera optical system, the measured distance between paired streaks on the film, and the time duration between flashes, it was possible to obtain an accurate value for the particle velocity.

Various components of the system will be discussed under the following categories: (1) camera-recording assemblage, (2) light bomb or illumination system, and (3) auxiliary-flow equipment needed to generate the particle flows. The critical component of the system was the light source, which required most of the development time and is covered in greatest detail.

#### CAMERA AND FILM UNIT

Because the event was shuttered by the light source, the requirements for the camera-shutter capabilities were not stringent; a relatively simple and inexpensive camera could be used. However, because of the short effective exposure times associated with the small particles moving at high-velocities, the lens and film became quite important.

##### Camera

The camera used in the tests was a 4 x 5 Speed Graphic press-type camera. In addition to 4 x 5 negatives and Polaroid-type films, the unit was equipped with a special back to accommodate regular Polaroid roll film.

The camera was modified to incorporate a nominal 10-to-1 magnification. The need for magnification to produce a visible streak was basically twofold: (1) streaks 1  $\mu$  wide would not be readily visible on the film unless they were widened by overexposure (halation), which is not usually desirable, and (2) it was required to allow the streaks to be long enough for an accurate measurement while keeping the physical distance that the particle had travelled to a minimum. A 10-to-1 magnification will produce a 1-inch streak on the film for a particle having travelled 1/10 of an inch. Keeping the physical displacement of the particle to a minimum is required to increase the probability that the particle will remain in focus, and to decrease the effects of axial velocity gradients on the measurement of the particle velocity.

The use of magnification has an inherent disadvantage because as the image on the film is increased in size, the amount of light per unit area is decreased. This loss of intensity is not, however, as great as image-size ratios would indicate because as the magnification is increased, the distance from the camera lens to the object (particles)

is decreased, which allows a larger solid angle of light to enter the camera.

### Camera Lens

The objective lens used with the Speed Graphic camera was a 75 mm f/1.9 Wollensak lens. It was chosen for these tests because it was the lowest f-number (highest speed lens) that was readily available. The f-number is defined as the ratio of the lens focal length to the diameter of the lens aperture. The theory concerning the f-number and the speed of the lens will not be discussed here since it can be found in almost any book on photography (Ref. 3). It should be stated, however, that the theory for the lens speed is defined for cameras where the distance of the object to the lens is much greater than the distance from the lens to the film. This corresponds to a camera demagnification. Because the camera system used in these tests has a nominal 10-to-1 magnification, the basic theory must be somewhat modified.

The 75 mm f/1.9 Wollensak lens used in these experiments and the majority of standard camera compound lenses were designed to be used in a camera with the lens much closer to the film than to the object, causing demagnification. Since the camera system used in these tests required magnification, it was observed that more light could be focused on the film by turning the lens around.

### Film

The choice of film-type was narrowed to films of high sensitivity because obtaining enough light was a major problem. Two Polaroid films and one 4 x 5 negative-type film were used in the tests.

Polaroid films were used because of their high sensitivity and the benefit of rapid development between tests. Tests performed with Polaroid Type 57 Land film ASA 3000 gave streaks of low brightness. To increase the brightness of the streaks, Polaroid Pola Scope Type 410 Land film with an equivalent ASA rating of 10,000 was used in the majority of the experiments. This film produced streaks about twice as bright as those obtained with the Polaroid Type 57 film. The Polaroid Type 410, however, was available only in rolls which reduced the overall size of the picture from 4 x 5 to about 3 x 4.

The 4 x 5 negative-type film used was Kodak Royal-X Pan Recording film which was developed for high contrast in D-19 developer for 5 minutes. This film and development produced a streak brightness between the brightness of the Polaroid Type 57 and the Polaroid Type 410 films.

## ILLUMINATION

The decision to frontlight the system and to precisely control the duration of the light pulse makes the light source extremely important in the following respects:

1. It should have sufficient intensity to expose a film in the order of 1 nanosec ( $10^{-9}$  sec) after the light has first been reflected from a  $1\mu$  particle.

2. The duration should be controlled so that repeatable data can be obtained. This indicates that for a total light pulse of 2 to  $5 \times 10^{-6}$  sec the deviation between tests should be less than  $1 \times 10^{-7}$  sec.

### Light Intensity

The high-intensity short-duration light sources that were considered were: (1) the spark, (2) the exploding wire, and (3) the explosive-shock rare-gas light bomb. System (3) was chosen for two reasons: (1) the explosive rare-gas system allowed a larger emitting surface for the light which, when focused, would allow a higher intensity over a larger field of view, and (2) with the explosive rare-gas system variations in pulse length and shape can be accomplished by simple geometric changes. The duration of the light pulse increases by increasing the thickness of gas that the shock must traverse.

The operation of an explosive rare-gas light source can be described as follows:

The detonation of an explosive charge forms a strong shock wave which propagates through gas contained within a cavity. The gas atoms are ionized by the shock and emit light when recombining with their electrons. Rare gases (argon, krypton, and xenon) produce a much higher light intensity for a given shock strength than other gases because none of the shock energy is lost in disassociating the molecules.

Argon is the gas most often used in explosive-gas light sources. However, work performed at Stanford Research Institute (Ref. 4) indicated that xenon and krypton, when shocked, emitted a higher light intensity than argon. Both krypton and argon were used in the Naval Ordnance Test Station experiments. Xenon was not tried because the increase in predicted intensity was not considered worth the additional cost.

The light-source or bomb that was designed and built is shown in Fig. 1 and an exploded view is shown in Fig. 2. The bomb was designed to produce a large solid angle of emitted light. This solid angle was dictated by both the diameter of the bomb and the amount of plexiglass required to attenuate the stress waves resulting from the detonation. The lens system on the front was used to condense the light in an effort to maintain a high light intensity on the field of view. Details on the light bomb and its construction are included in Appendix B.

To determine if this light bomb would produce the required light intensity, it was tested under the conditions in which it was to be used. Streaks in a supersonic helium flow (about 3,000 ft/sec) were photographed using aluminum, aluminum oxide, magnesium oxide, and tungsten particles as small as  $2\mu$ . This light intensity test in no way justifies a statement that the light source will reach the upper limit for which it was built ( $1\mu$  particles traveling at 5,000 ft/sec). It is believed, however, that if higher intensity light is required the present system can be optimized to reach this upper limit.

#### Controlled Light Pulse

Producing a controlled, repeatable light pulse developed into a more difficult problem than obtaining sufficient light intensity. Because the pulse duration had to be about  $3\mu$  sec the rise and fall times had to be extremely short to approximate a square wave. To check the characteristics of the light pulse, the light bomb output was photographed using a Beckman Whitley Model 168 streak camera. The light bomb tests were set up with the streak camera looking straight into the light source. The camera was aimed down the light bomb axis through the gas gap and focused on the circular explosive surface. The camera slit was adjusted so that the distance from the centerline of the explosive to the outer edge of the explosive was photographed as the ordinate on the film and time was recorded as the abscissa. The approximate shape of the detonation wave and the time of the light pulse can be determined by this method. The detonation wave begins to emit light on reaching the explosive-gas interface. A curved detonation wave will first reach the explosive-gas interface at the centerline and with time, extend to the outer edge. The initial light transient would be curved on the film representing the curve of the detonation wave. The light would then continue until the shock had traversed the gas gap.

The first tests in which the light-bomb output was photographed showed, as would be expected by considering the detonator as essentially a point-source initiator, that the detonation wave was curved. This resulted in a light pulse with an unacceptable long rise time. Because small explosive plane-wave generators are expensive, a second tetryl pellet was placed behind and in contact with the first pellet to give the explosive a longer length. This longer length reduced the curvature of the detonation wave at the explosive-gas interface to a tolerable value.

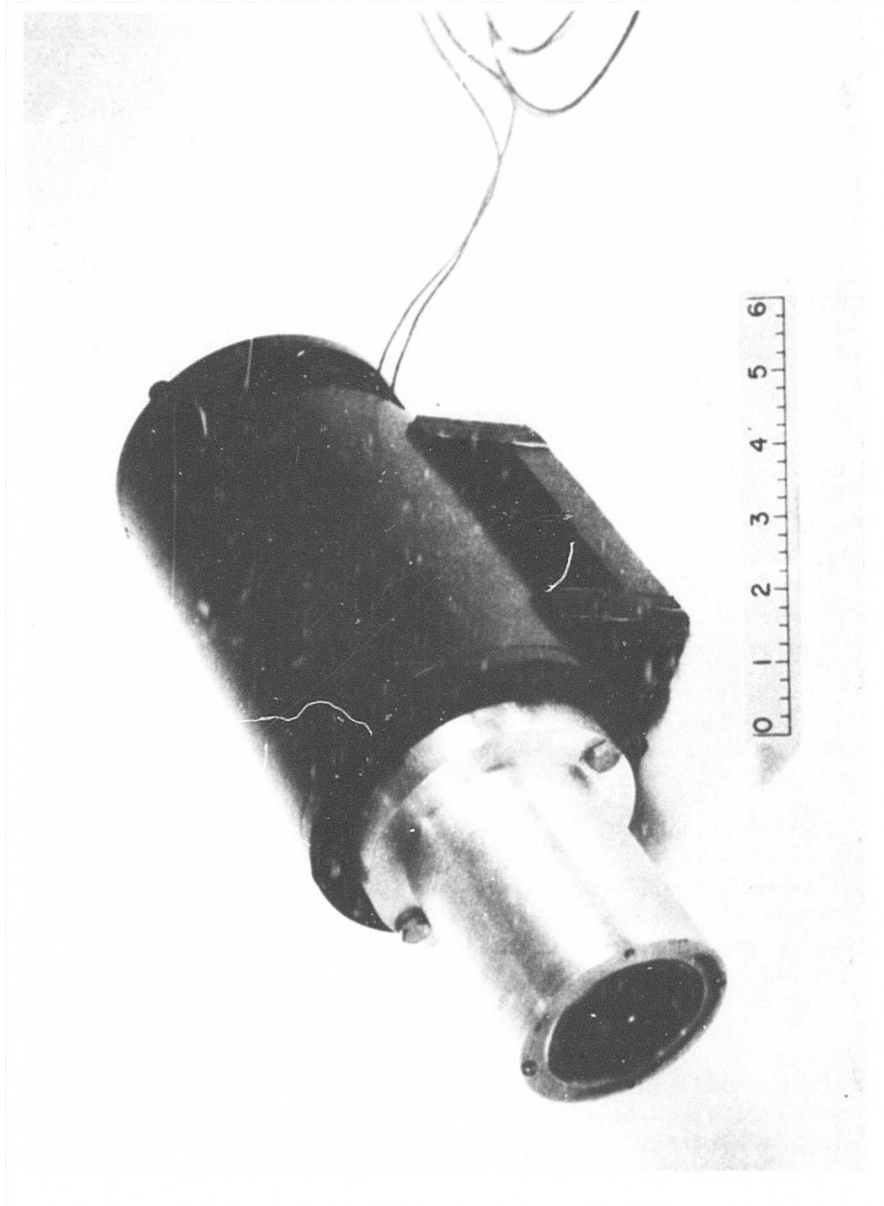


FIG. 1. Explosive Rare-Gas Light Bomb.



Explosive rare-gas light sources often use a metal buffer or piston between the explosive and the gas (Ref. 5). The piston shocks the gas as it moves and aids in producing a pulse with short rise and fall times. Tests with various buffer materials and thicknesses indicated that the buffer greatly reduced the light intensity. The metal buffer was eliminated from the system because it was important to obtain the highest light output possible.

The use of two tetryl pellets resulted in a sharp rise time; the problem remaining was to obtain a rapid termination of the light pulse. The first tests showed that the light terminated rather slowly after the shock had traversed the gas gap and impacted the plexiglass front. Other research performed at the Naval Ordnance Test Station indicated that the light from various gases could be extinguished rapidly by coating the gas-plexiglass interface with nitrocellulose, Saran Wrap, or even Duco cement (Ref. 6). However, tests with this system using relatively large gas gaps and no buffering pistons indicated that these materials failed to extinguish the light at the required rate.

As tests continued using various techniques to rapidly terminate the light pulse, a new tangent to the problem was also pursued. It had been shown by other investigators in this field that the emitted light can be made to pulse many times (Ref. 7). Therefore, by obtaining a rapid rise of two pulses, accurate time can be measured from the beginning of the first pulse to the beginning of the second pulse.

The attempts to rapidly terminate a single light pulse were stopped when the two-pulse system began showing repeatable results. The two-pulse system adopted used one gap containing a rare gas followed by one gap containing air. The air gap allowed the light intensity generated by the rare gas to decrease to a low level. The second and shorter pulse resulted when the shock wave impacted against the air-plexiglass interface (Fig. 2). Figure 3 shows a Beckman Whitley streak photograph of the two-pulse output. It should be noted that both pulses have rapid rise times as shown by their sharp and relatively straight fronts. Termination of both pulses is rather slow, but this does not hamper accuracy since measurements are taken from the beginning of the first pulse to the start of the second. The first pulse was made of longer duration than the second to avoid confusion in identifying and measuring actual particle streaks in the flow photographs.

Nine light tests were run using the streak camera to determine the repeatability of the two pulses. The results showed that the average time from the start of the first pulse to the beginning of the second was  $3.14 \times 10^{-6}$  sec. The standard deviation from this value was  $\pm 5 \times 10^{-8}$  sec which results in a fractional standard deviation of 1.6% of the total time.

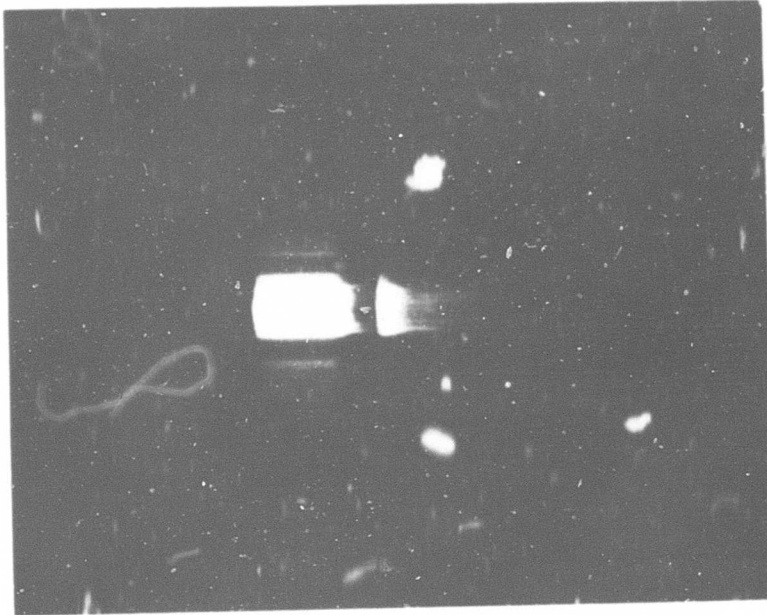


FIG. 3. Streak Camera Record Showing Light Output Pattern for Explosive Rare-Gas Light Bomb Arranged for Dual Pulse Operation.

#### FLOW APPARATUS

The flow apparatus was kept as simple as possible because the major emphasis was placed on developing photographic velocity-measurements technique. The flow apparatus was required only to produce a supersonic gas flow containing dispersed solid-metal particles.

The working medium of gas used was helium which was chosen because of its high speed of sound and its safety as an inert gas. The speed of sound in helium is about 3,000 ft/sec at room temperature.

The nozzle (Fig. 4) was designed for two-dimensional flow and was made by sandwiching two contoured micarta plates between two plexi-glass plates. It was designed with transparent walls to allow observation of irregularities in particle mixing and flow. Basically, the sonic-type nozzle has a primary (large hose) inlet for helium, a secondary inlet for helium with dispersed particles, and taps for chamber and throat pressures.



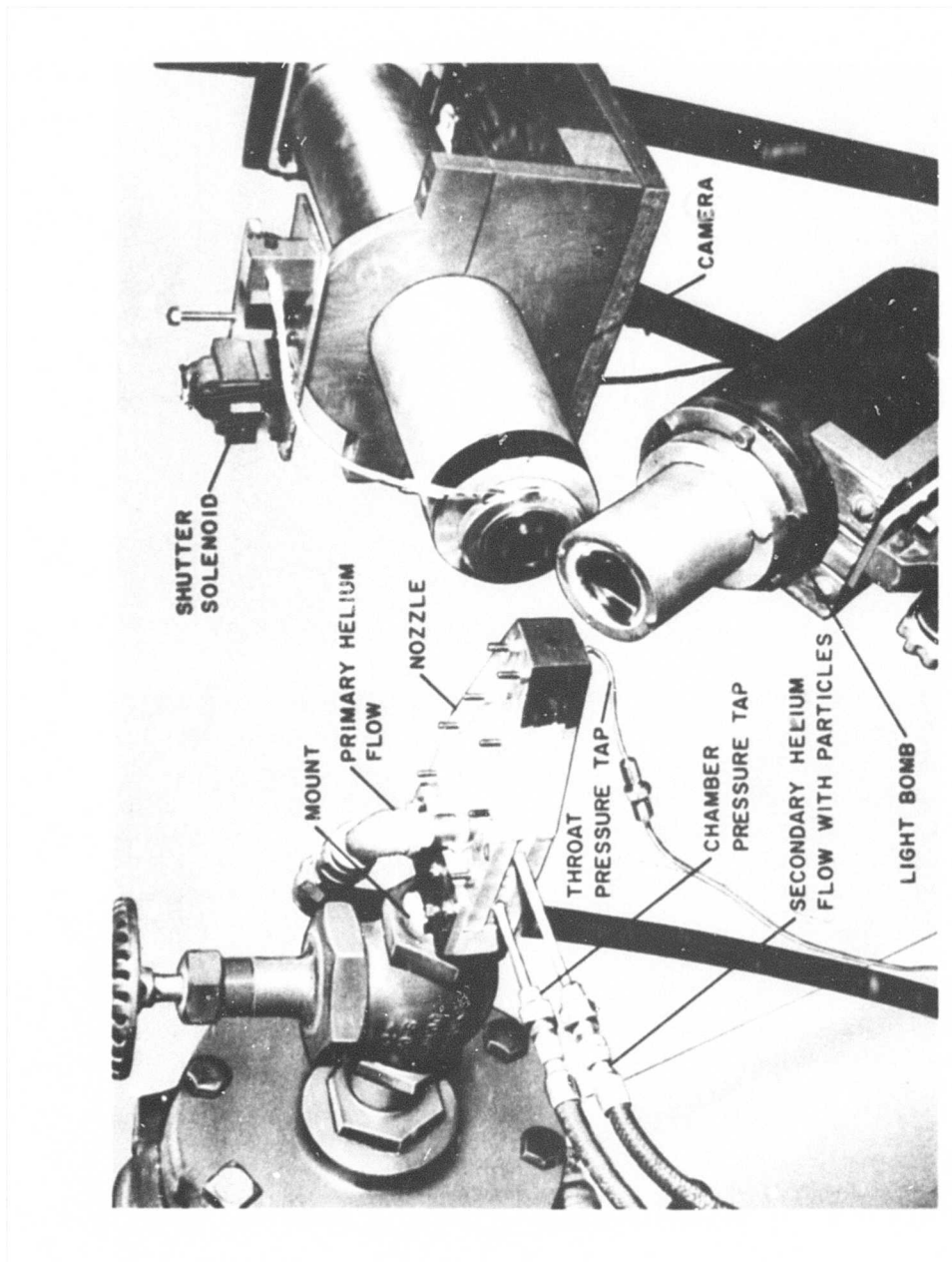


FIG. 4. Alignment of Nozzle, Light Bomb and Camera.

The problem of breaking up particle clumping could not be solved solely by the kinetic forces of the gas. A particle generator (Fig. 5) was designed to aid in dispersing individual particles in the gas stream. The combination of beating the particles through the cotton bag with the action of the kinetic forces of the gas eliminated the problem. There existed, also, a measure of control over the number of particles in the flow because the DC motor which drives the beater allowed a variable rpm.

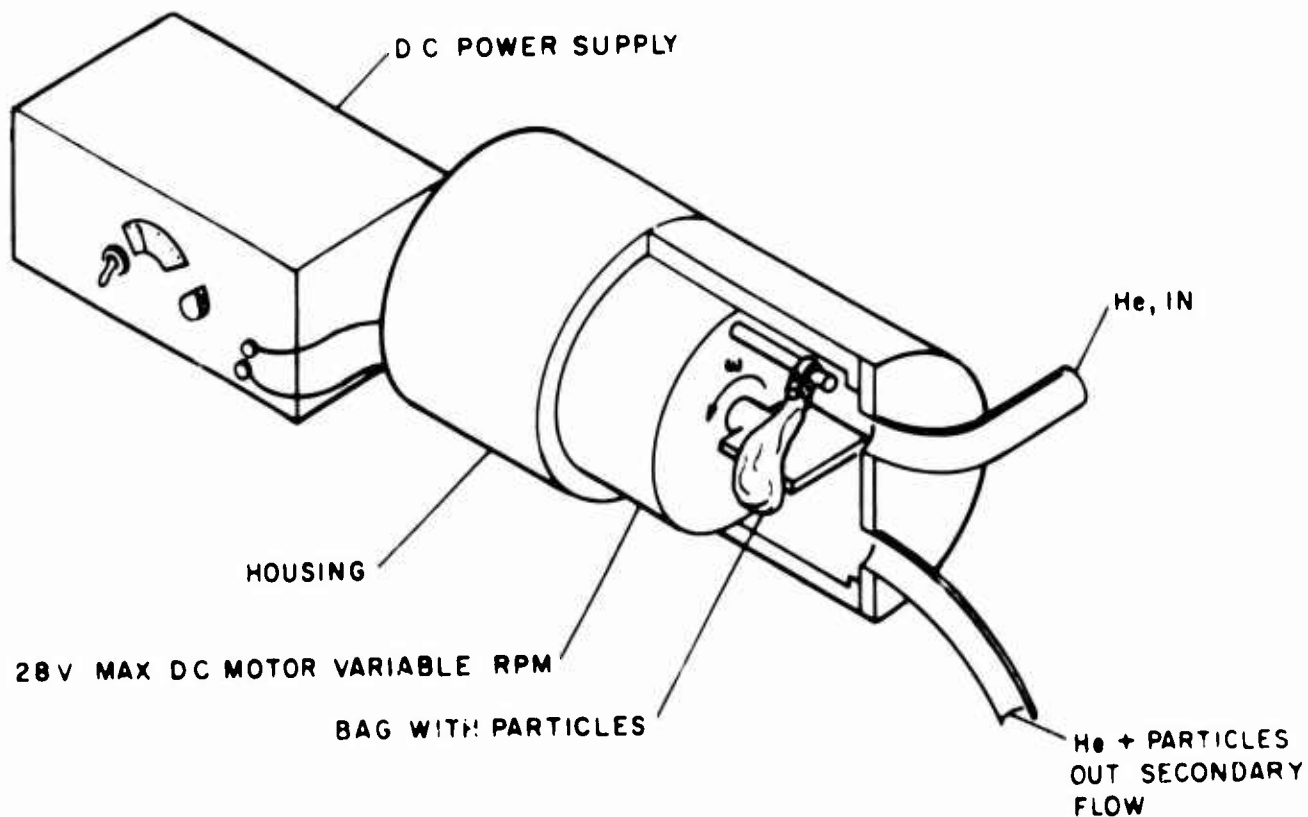


FIG. 5. Particle Generator.

## PARTICLES

Various size particles and materials were used in checking out the system and running photographic and light tests.

Particles ranging from 1 to  $10\mu$  are available commercially; however, the particle sizes are usually nominal. Powders of a stated  $5\mu$  nominal size may range from submicron to  $30\mu$  diameter with the maximum distribution about  $5\mu$ .

To obtain significant velocity data for various particle sizes, the problem existed of obtaining particles in much closer distribution (a spread of only 1 or  $2\mu$ ). Added to this problem was the need for spherical particles to eliminate the parameter of particle shape and to approximate the shapes that liquid particles have in a hot rocket motor. Various

commercial suppliers were contacted and confronted with these size restrictions with no positive results. An attempt was made here to separate aluminum particles with BMC (Buckbee Mear Co.) Micro Mesh sieves. These sieves for particles of 5, 10 15 20, and  $25\mu \pm 2\mu$  were easily clogged and the process was very slow. The results were poor and are discussed in some detail in the section on Particle Velocity Measurement.

INTEGRATED SETUP

The various components of this system were set up as shown schematically in Fig. 6. The sonic nozzle was fed by two helium gas bottles; the primary flow was controlled by a solenoid valve connected to a simple control box; the secondary helium flow was connected through the particle generator to the nozzle. Both the helium regulator and the particle generator beater speeds were controlled by hand so that some control over the particle density in the flow could be maintained. The camera shutter and the light bomb were controlled electrically from the control box.

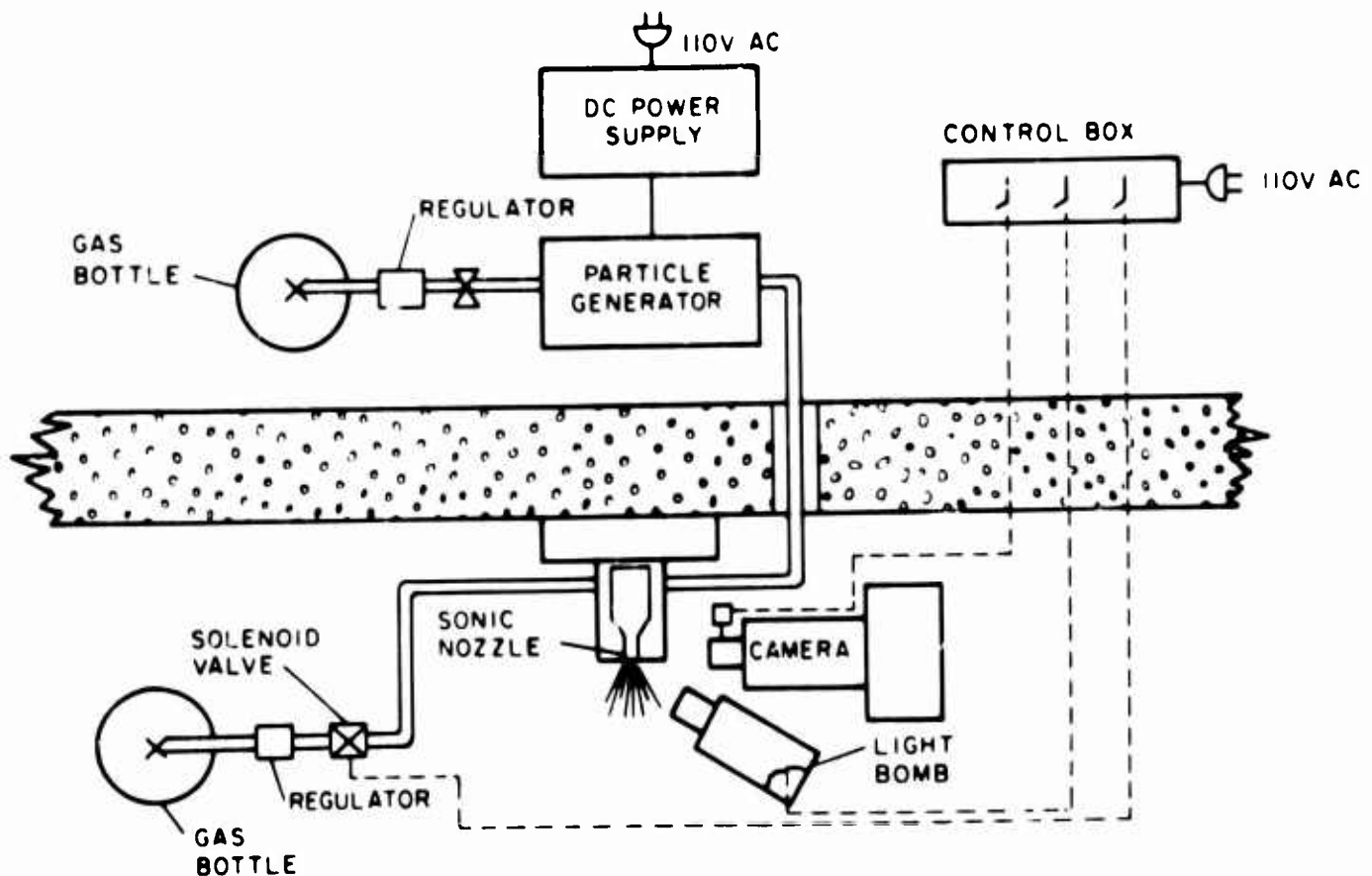


FIG. 6. Test Arrangement for Particle Velocity Tests.

## PRETEST ALIGNMENT

The alignment of the various parts was critical as with most optical systems. The components of the system (Fig. 7) are basically the camera, light bomb, and nozzle. To simplify the alignment a focusing plate with a 1 mm grid was inserted into the nozzle exit along the axis of flow. A light bulb was placed in the light bomb before insertion of the explosive. The light bomb was then aligned to cover the field of view and to give maximum light on the focusing plate. This required the front lens on the light bomb to be placed about one focal length from the axis of the flow. The camera was then focused on the focusing plate with care taken that the field of view of the camera was the same as the field covered by the light source. The explosive, detonator, and back plate were then carefully placed in the light bomb. The assembling of the light bomb itself is discussed in Appendix B.

After the system components were carefully aligned, the camera lens was set and the film inserted into the camera. When placing the film in the camera, the lights were kept as low as possible because of the high sensitivity of the film. The connecting of the detonator leads to the shunted firing line was the last step in the preparation of the system for testing.

## FIRING SEQUENCE

The test procedure was simplified by conducting the tests in the dark, making it unnecessary to incorporate fast camera shutters and complicated synchronization. The tests proceeded as follows:

- 5 sec: Primary-helium and secondary-helium particle flows initiated
- 2 sec: Camera lens opened
- 0 sec: Light bomb fired
- +1 sec: All systems deactivated

## PARTICLE VELOCITY MEASUREMENTS

During the program a total of 45 tests was run in which photographs were taken of the particle flows. Thirty-five of these tests were expended in the process of developing the technique. The remaining 10 were run under controlled conditions to demonstrate the capabilities of the system and to secure measurements of particle velocities for preliminary comparison with theoretical data.

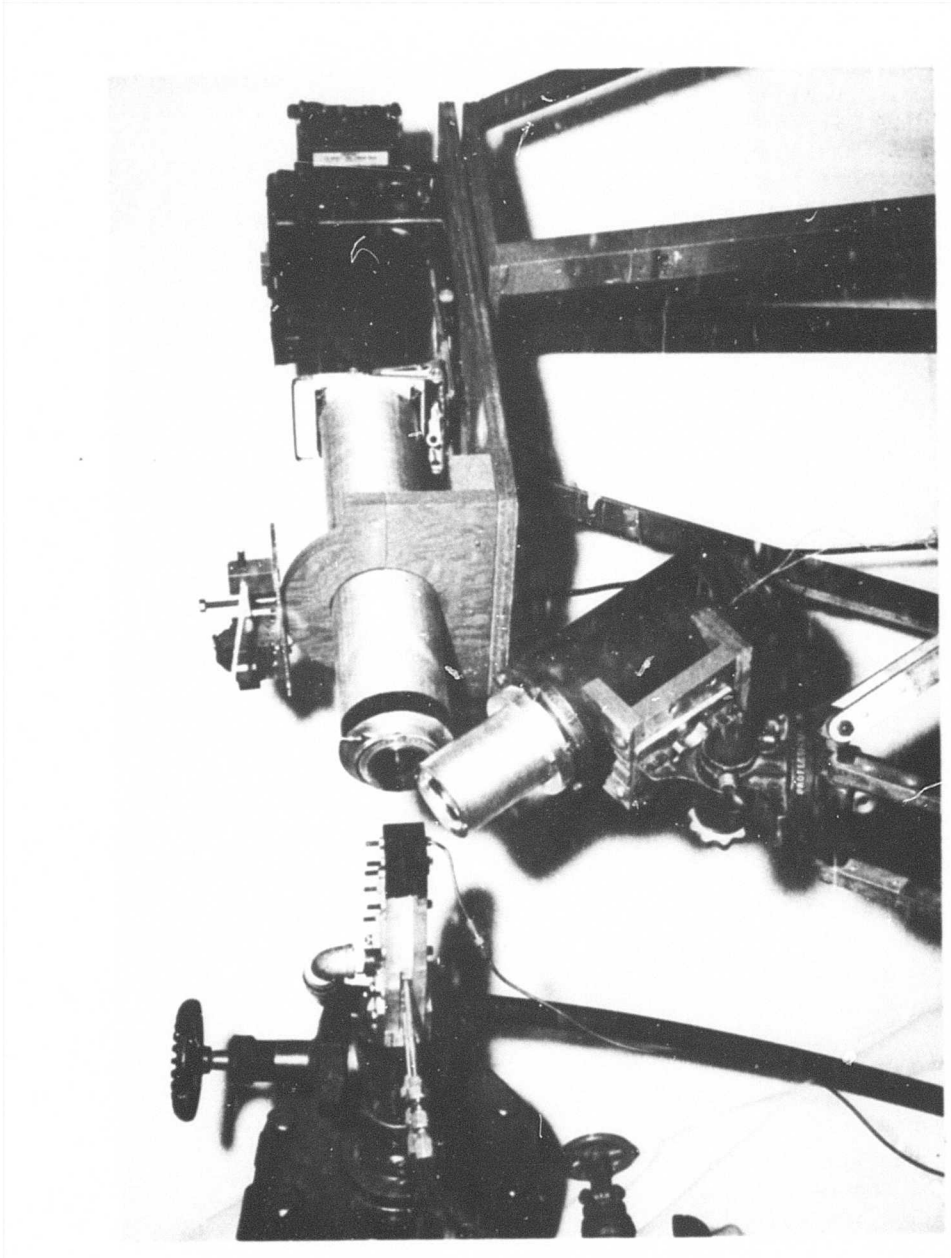


FIG. 7. Particle Measurement Test Setup.

## EXPERIMENTAL EQUIPMENT

The development of the equipment used in these tests was discussed previously. The same modified Speed Graphic camera used in preliminary tests was used in combination with the roll-type Polaroid back and ultra-high-speed Polaroid 410 film. Pictures taken of the focusing grid before each shot established the magnification of the system at a constant value of 9.51X.

The light bomb was arranged for two-pulse operation using krypton and air in the dual gaps. Two 1/2-inch tetryl pellets were used in series to provide the detonation wave. Figure 7 shows the placement of the bomb with respect to the camera and nozzle.

## FLOW FIELD STUDIES

It was necessary to establish a fairly constant gas-velocity field in which to take pictures of the particles for the data runs. A series of preliminary tests was run with the nozzle system to determine the chamber pressure needed to just achieve sonic flow at the nozzle throat (which, in this case, is also the nozzle exit). Under these circumstances the exit (throat) static pressure equals the ambient pressure and a short region is established directly downstream from the nozzle exit in which the gas maintains a constant velocity equal to the sonic value (2,900 ft/sec for helium at nozzle-exit static temperatures).

To determine the necessary chamber pressure, measurements were taken of both the chamber and nozzle (exit) pressures and the ratio of the two pressures plotted as a function of pressure. When the flow became sonic in the throat, the flow was choked and the ratio of chamber pressure to exit pressure became constant. Although this transition point could be calculated theoretically, it was decided that the transition point should also be determined experimentally. With the high value of specific heat ratio associated with helium, the dissipative processes within the flow become larger and the error in the calculated value increases. The critical chamber pressure was found to be a little over 30.5 psia at an ambient pressure of 13.5 psia; this is about 3 psi higher than predicted by theory.

Tests showed that the number density of particles within the stream was quite low and it was assumed (based on theoretical data) that in the region of interest the gas velocity would be essentially unaffected by the presence of the particles.

## PARTICLE PROBLEMS

Alcoa 1230 aluminum powder was chosen for use in the particle velocity measurement studies because of its appropriate size distribution and

the nearly spherical shape of the particles. As mentioned previously it was very difficult to obtain powders having narrow size distributions. A series of Buckbee-Near Micromesh sieves was used to further break down the aluminum powder into four fractions: sub- $10\mu$  (fraction 1), 10 to  $15\mu$  (fraction 2), 15 to  $20\mu$  (fraction 3), and 20 to  $25\mu$  (fraction 4).

The particle velocity data of the tests did not correlate well with the particle groupings. Fortunately, samples of the particles in the flow had been collected before each test series by passing a plastic slide, coated with fresh Duco cement, through the gas-particle stream. Photomicrographs of the particles were taken with an American Optical Company Model 2400 metallograph microscope at a magnification of 200X (Fig. 8-11). By measuring the diameter of the particles in each photograph, it was possible to determine an approximate size distribution (Fig. 12). Although the sub- $10\mu$  group (fraction 1) appeared to be the size expected as a result of the filtering process, the other three fractions appeared to be substantially larger than thought at first. The mean particle diameter of both fractions 2 and 3 was about  $25\mu$  instead of lying in the 10 to  $15\mu$  (fraction 2) and the 15 to  $20\mu$  (fraction 3) ranges. The mean diameter of fraction 4 was about  $36\mu$  instead of lying in the expected 20 to  $25\mu$  distribution. It was very difficult to wash out all the fine material from fractions 2, 3, and 4; thus, the distribution curves for these fractions in Fig. 12 will have an upward trend in the sub- $3\mu$  range. A second exposure (Fig. 8) was taken on the same film in order to superimpose a picture of a known-size reticle. The distance between the lines in the reticle was equal to 0.005 inch. With this it was possible to verify the camera magnification of 200X.

#### EXPERIMENTAL ARRANGEMENT AND PROCEDURE

The experimental arrangement of equipment and the procedures used during the tests were essentially the same as were used during the development studies. These are described in the section titled Integrated Setup.

#### RESULTS AND DISCUSSION

The data photographs are shown in Fig. 13-22. Four tests were run using the smallest particles (fraction 1) and two tests each with the other three fractions. Detail on some of the smaller streaks has been lost in reproduction. The pictures are sufficiently good, however, to show the dual streak characteristics of the larger particles. There is a long streak caused by the krypton flash followed by a much shorter, less intense streak, resulting from compression effects as the shock wave impacts the air-plexiglass interface. In many cases this resembles a horizontal exclamation point.

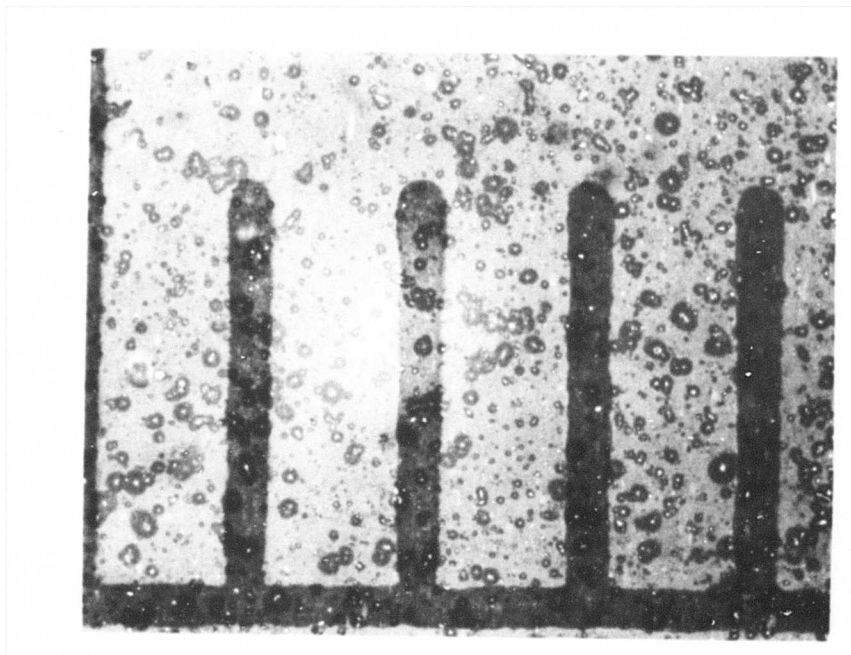


FIG. 8. Photomicrograph of the Particles in Fraction 1 (200X Magnification).

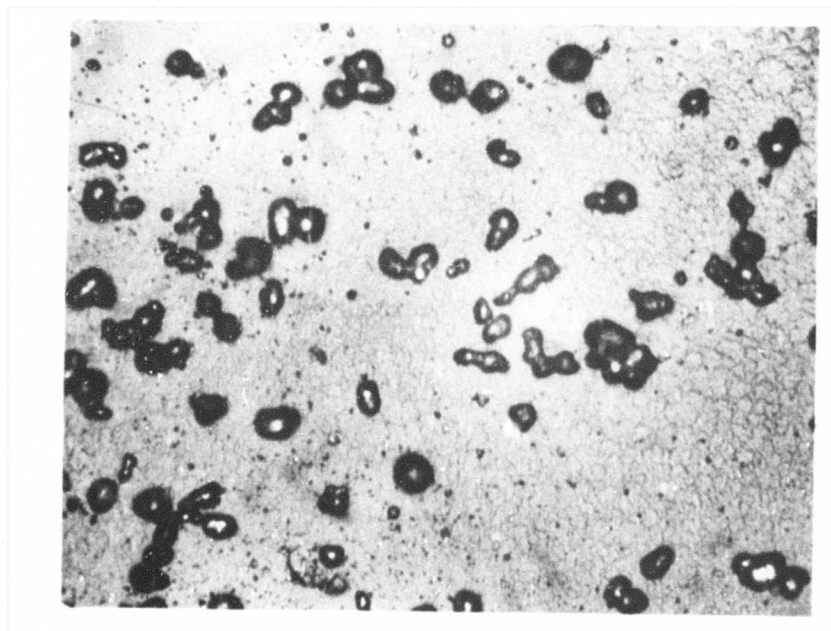


FIG. 9. Photomicrograph of the Particles in Fraction 2 (200X Magnification).



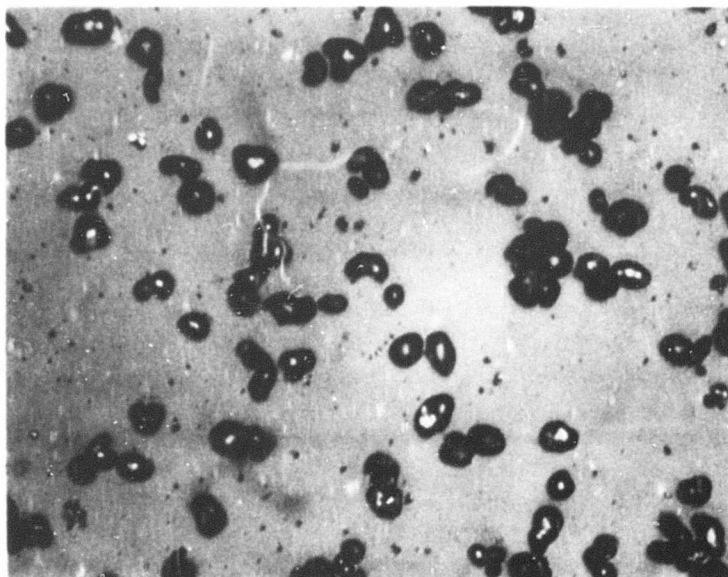


FIG. 10. Photomicrograph of the Particles in Fraction 3 (200X Magnification).

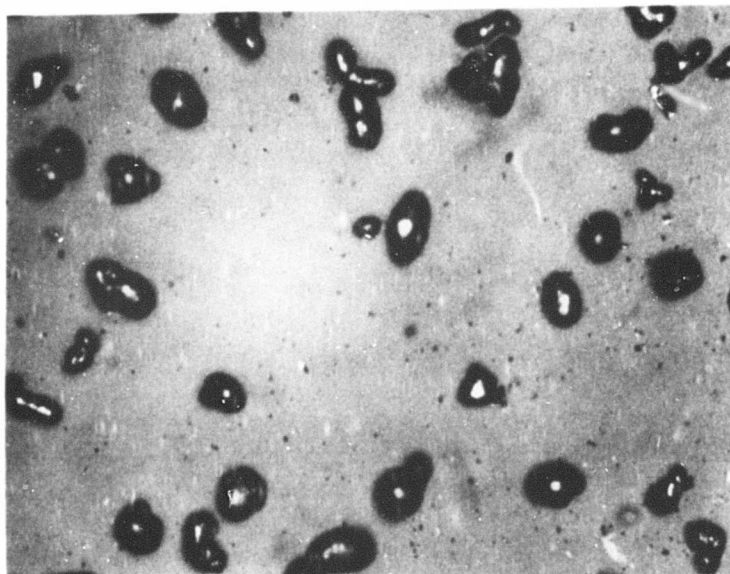


FIG. 11. Photomicrograph of the Particles In Fraction 4 (200X Magnification).

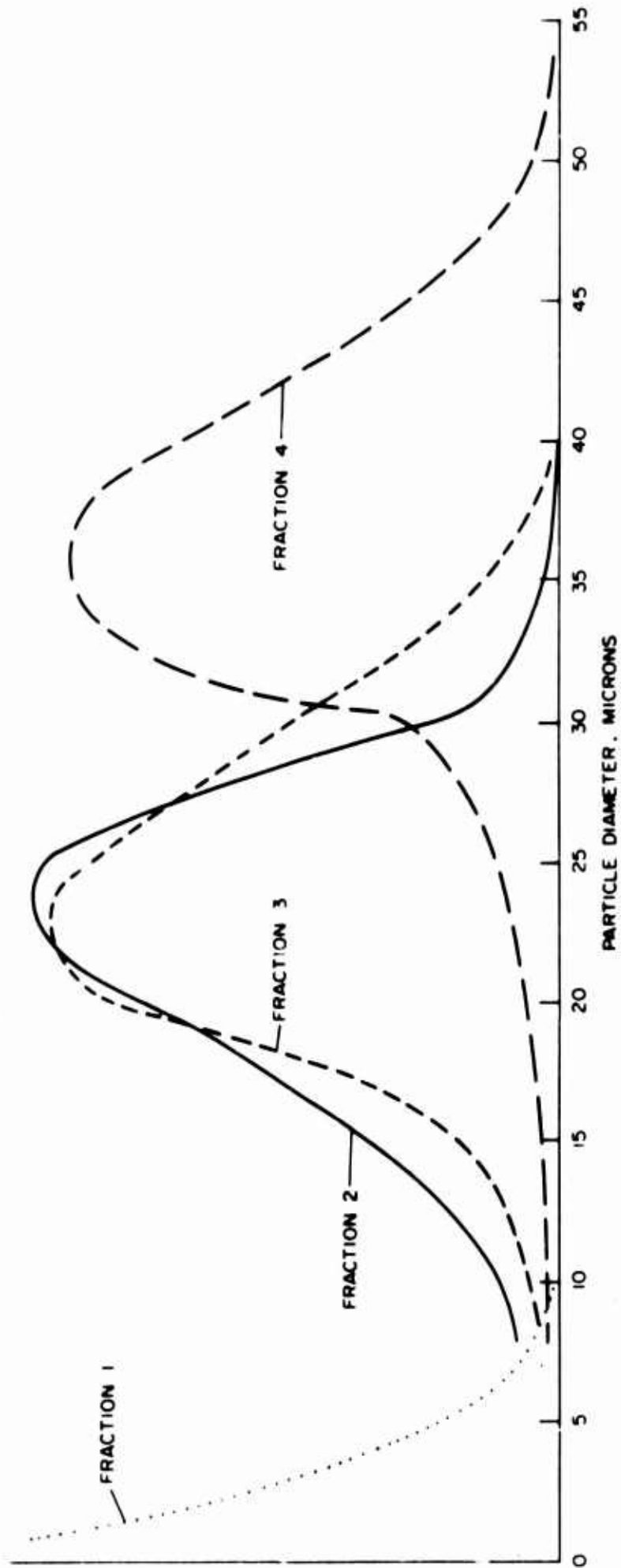


FIG. 12. Size Distribution for Aluminum Powder Fractions Used in Particle Velocity Measurements.

The width of the streaks can be seen to increase as the particles become larger from series to series. This is caused by two effects: (1) the obvious geometric effect of a larger particle leaving a wider track; (2) the fact that the larger, slower moving particles reflect much more light which results in overexposure of the film and halation. This latter effect is especially noticeable in Fig. 21-22. After Fig. 21 was photographed the lens iris was closed down from  $f/2.8$  to  $f/8$  for Fig. 22. The decrease in light transmission dramatically reduced the size of the particle trace width. Thus, it would be difficult to determine particle size from streak width with any degree of accuracy (this has been attempted by several experimenters in the field of metal combustion). It should be noted that the large blotches of light shown in many of the pictures also result from the halation of large slow-moving particles outside the limits of sharp focus.

It is also interesting that in several cases the light is reflected from the particle in a cyclical manner, producing a trace that looks like a string of beads. A good example of this is shown in the trace above the No. 6 flag in Fig. 19. It is not caused by variations in the light source, because not all the streaks show this phenomenon. One speculation is that the particle surface is not uniform and in some way rotation or vibration has been induced. It is possible that the aluminum particle may have impacted on some surface during its journey into the through the nozzle, and developed a flat surface. Through aerodynamic forces a spin could develop on the particle which would, in turn, result in a variation in the light reflected as the flat spot rotates in and out of the critical reflection point. However, for this to be true, it would be necessary for the particle in Fig. 19 to be either rotating or vibrating at a rate of about 3 million cps. It can be seen from the foregoing that surface irregularities could also result in streak-width variations, which would further cast doubts on the validity of determining particle size through the use of streak widths.

It should be noted that not all the particles start out clearly, and in many cases the second, shorter trace, may be missing completely. This results primarily from the lower intensity of the secondary streak and the very shallow depth of field caused by the large lens opening used, the large magnification incorporated, and the very small allowable circle of confusion. Thus, particles that trace trajectories at angles as shallow as 1 degree to the plane of interest can go in and out of focus during the time it takes to traverse one-path length. This actually is a real benefit to the experiment in that errors, resulting from velocity components at right angles to the measurement plane, are nearly eliminated.

The numbers on the photographs indicate the points chosen for data evaluation; the assigned numbers can be correlated with the tabulated data given in Table 1. The streaks were measured with a 6X comparator to an accuracy of  $\pm 0.01$  inch. To qualify for consideration, the streak

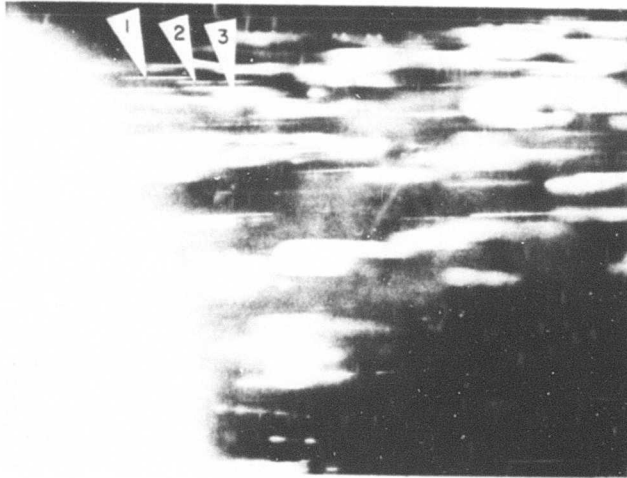


FIG. 13. Streak Photographs of Small Particles in a 2,900 ft/sec Helium Gas Stream. Particle Fraction 1. Run D1.

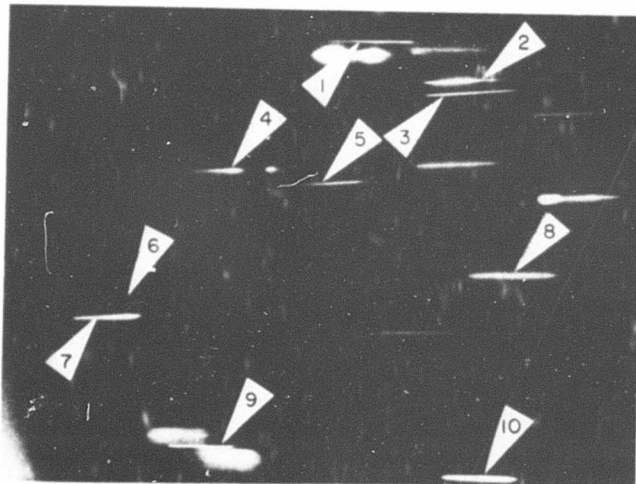
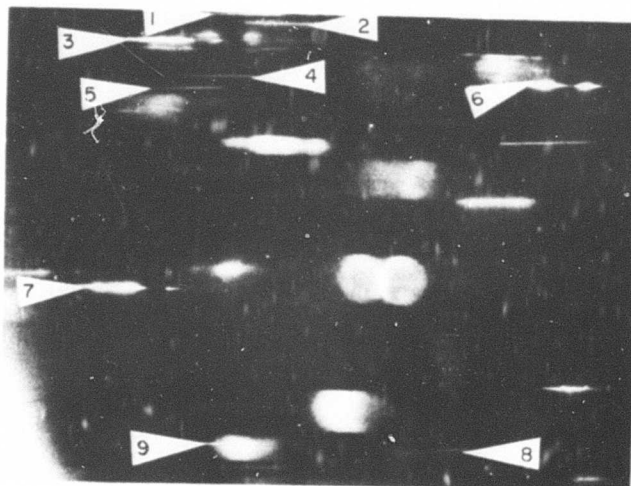
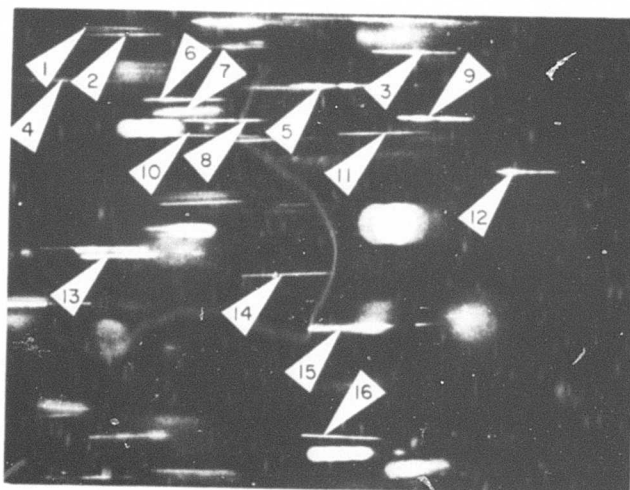


FIG. 14. Streak Photographs of Small Particles in a 2,900 ft/sec Helium Gas Stream. Particle Fraction 1. Run D2.



**FIG. 15. Streak Photographs of Small Particles in a 2,900 ft/sec Helium Gas Stream. Particle Fraction 1. Run D3.**



**FIG. 16. Streak Photographs of Small Particles in a 2,900 ft/sec Helium Gas Stream. Particle Fraction 1. Run D4.**

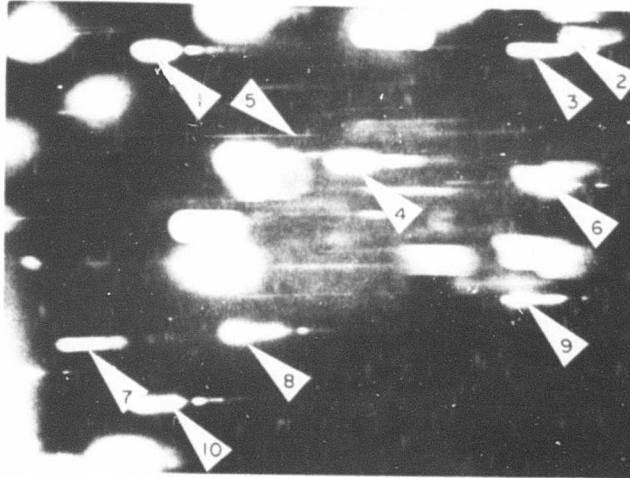


FIG. 17. Streak Photographs of Small Particles in a 2,900 ft/sec Helium Gas Stream. Particle Fraction 2. Run D5.

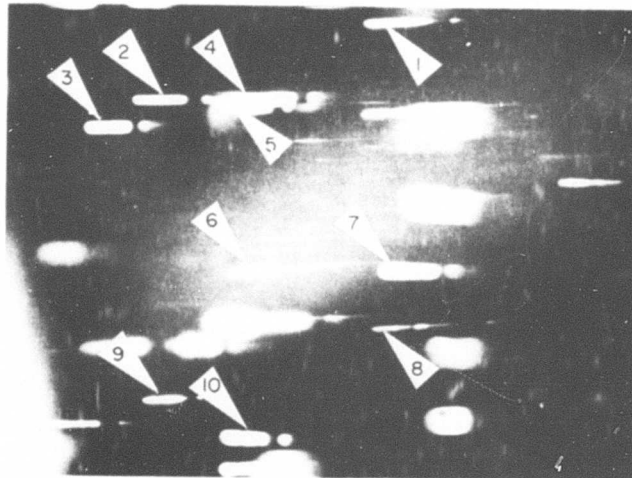


FIG. 18. Streak Photographs of Small Particles in a 2,900 ft/sec Helium Gas Stream. Particle Fraction 2. Run D6.

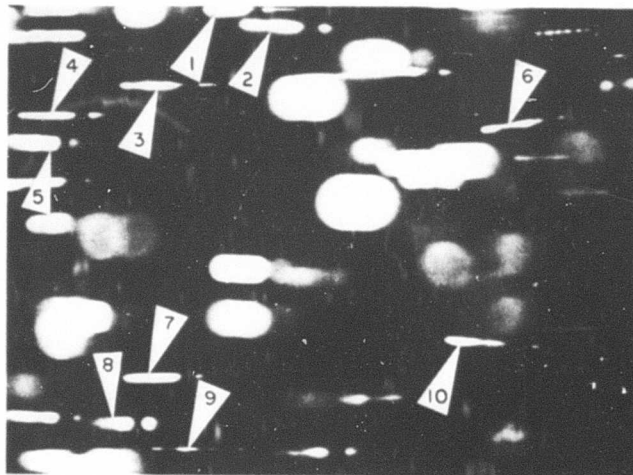


FIG. 19. Streak Photographs of Small Particles in a 2,900 ft/sec Helium Gas Stream. Particle Fraction 3. Run D7.

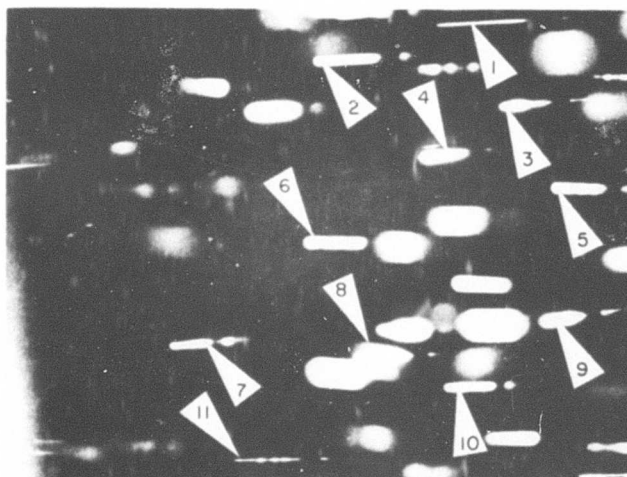


FIG. 20. Streak Photographs of Small Particles in a 2,900 ft/sec Helium Gas Stream. Particle Fraction 3. Run D8.

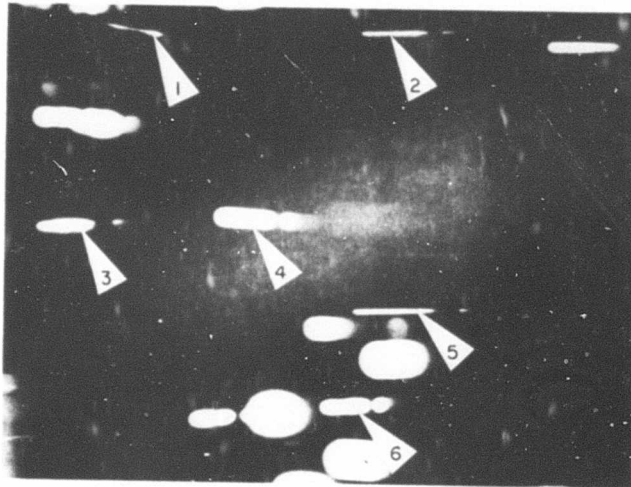


FIG. 21. Streak Photographs of Small Particles in a 2,900 ft/sec Helium Gas Stream. Particle Fraction 4. Run D9.

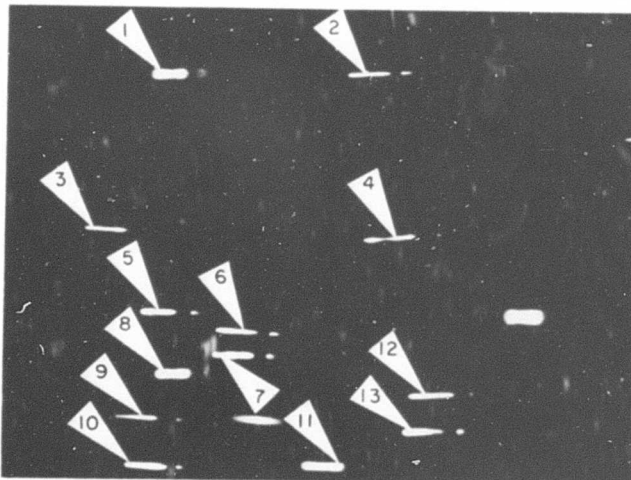


FIG. 22. Streak Photographs of Small Particles in a 2,900 ft/sec Helium Gas Stream. Particle Fraction 4. Run D10.



had to possess relatively distinct starting points for both sections of the trace. Measurements were taken from the start of the first streak to the start of the second.

Knowing the measured distance between streaks,  $s$ ; the magnification of the lens system,  $m$ ; and the time duration between the onset of the two streaks,  $t$ ; the particle velocity can be calculated from

$$v = \frac{s}{mt}$$

TABLE 1. Particle Measurement Data

Test No.	Streak No.	Measured velocity, ft/sec	Test No.	Streak No.	Measured velocity, ft/sec	
D1	1	1,770	D4	5	2,020	
	2	1,940		6	2,050	
	3	1,830		7	1,750	
D2	1	2,080		8	2,000	
	2	1,910		9	1,830	
	3	2,330		10	2,270	
	4	1,550		11	2,410	
	5	2,110		12	1,500	
	6	2,110		13	2,080	
	7	1,550		14	2,220	
	8	2,130		15	1,770	
	9	1,660		16	1,890	
	10	1,770		D5	1	950
D3	1	2,020			2	1,280
	2	1,800			3	1,300
	3	1,440			4	1,000
	4	2,270	5		2,610	
	5	2,190	6		1,300	
	6	1,800	7		1,530	
	7	1,500	8		1,280	
	8	2,580	9		1,330	
	9	1,940	10		1,110	
D4	1	2,020	D6	1	1,390	
	2	2,020		2	1,140	
	3	1,860		3	890	
	4	1,390		4	1,220	
		5		1,190		

TABLE 1. (Contd.)

Test No.	Streak No.	Measured velocity, ft/sec	Test No.	Streak No.	Measured velocity, ft/sec
D6	6	1,190	D8	8	1,220
	7	1,330		9	1,030
	8	1,890		10	1,000
	9	920		11	1,410
	10	970			
D7	1	970	D9	1	1,470
	2	1,300		2	1,330
	3	1,300		3	1,220
	4	1,160		4	1,050
	5	1,000		5	1,750
	6	1,250		6	860
	7	1,160	D10	1	720
	8	1,140		2	860
	9	1,440		3	920
	10	1,410		4	1,220
D8	1	2,050	5	830	
	2	1,390	6	890	
	3	1,160	7	890	
	4	1,110	8	780	
	5	1,140	9	1,000	
	6	1,190	10	830	
	7	890	11	920	
			12	1,000	
			13	890	

In all 10 cases, as noted previously, the magnification was 9.51 and the time duration was 3.14 sec between flashes.

The particle velocity data for the various runs are given in Table 1. The fractional standard deviations varied from 1.5% for the highest velocities to 3.2% for the lowest ones. The particle velocities are presented graphically in a bar-type plot (Fig. 23) which also shows the velocity distribution obtained with the different fractions. The larger particles (fraction 4) are traveling at the slower velocities (between 800 and 1,000 ft/sec). The smallest particles (fraction 1) were traveling the fastest and ranged from 1,700 to 2,600 ft/sec. Fractions 2 and 3 both appear to be moving at about the same velocity. Previous to the discovery that the particle fractions were not in the ranges indicated by the filtering processes, this data caused considerable concern. However, as noted previously (Fig. 12), the size distributions of the

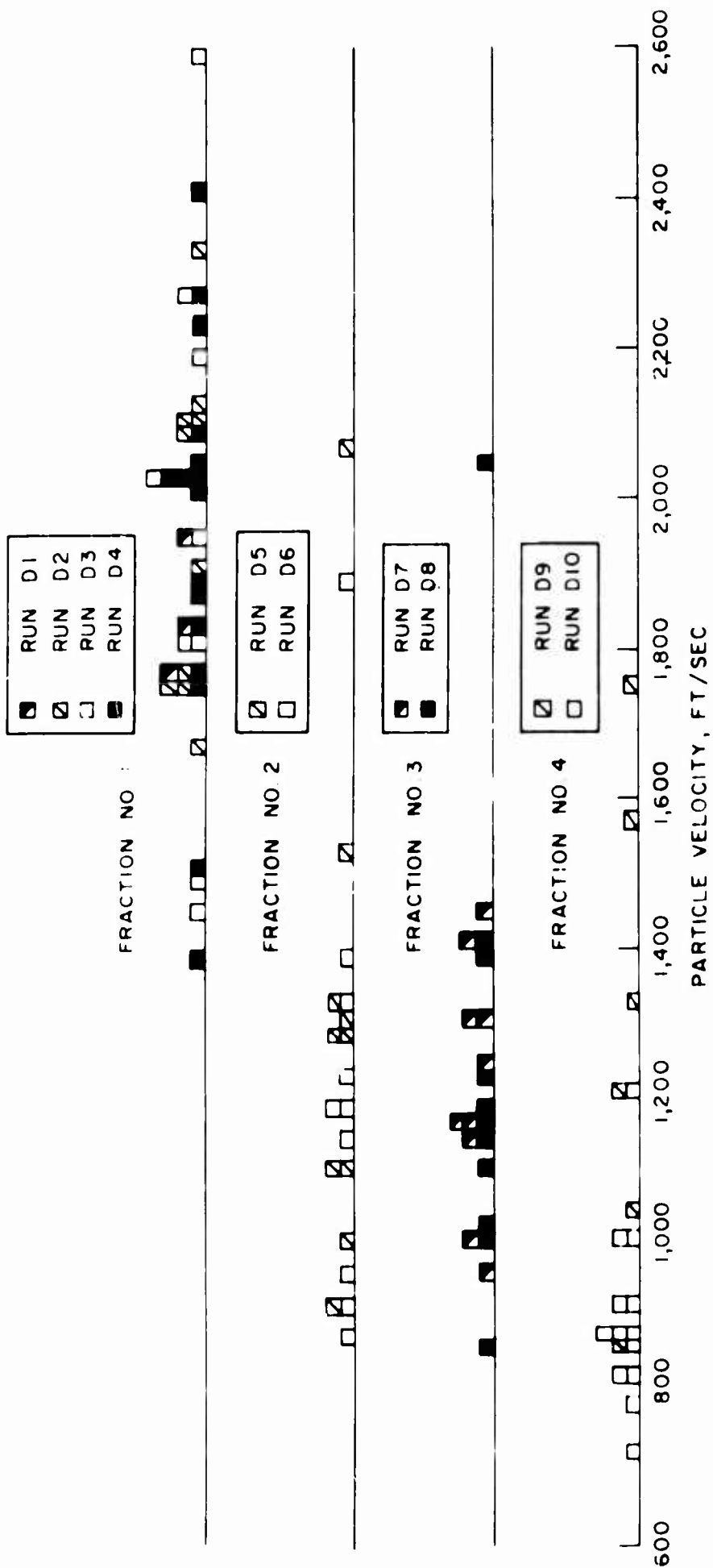


FIG. 23. Particle Velocity Distribution for the Various Aluminum Powder Fractions (2,900 ft./sec Helium Carrier Gas).

two fractions turned out to be very close, which explains the similarity in velocity distributions for the two fractions.

The particle size and velocity distributions were compared for the different fractions. A range of possible particle sizes corresponding to discrete, selected values of particle velocity was obtained by noting the end points and mean values of both distribution curves (Fig. 12 and 23) for each of the particle fractions. This was done independently by both authors to obtain two sets of measurements that could be compared, since the correlation process depends, to a large extent, on judgment. The resulting velocity figures were then normalized by dividing the particle velocity by the gas velocity (2,900 ft/sec) and the resulting ratio plotted against particle size (Fig. 24). The widths of the horizontal lines are an indication of the uncertainty of the data. A curve has been drawn through the data to better demonstrate the trend.

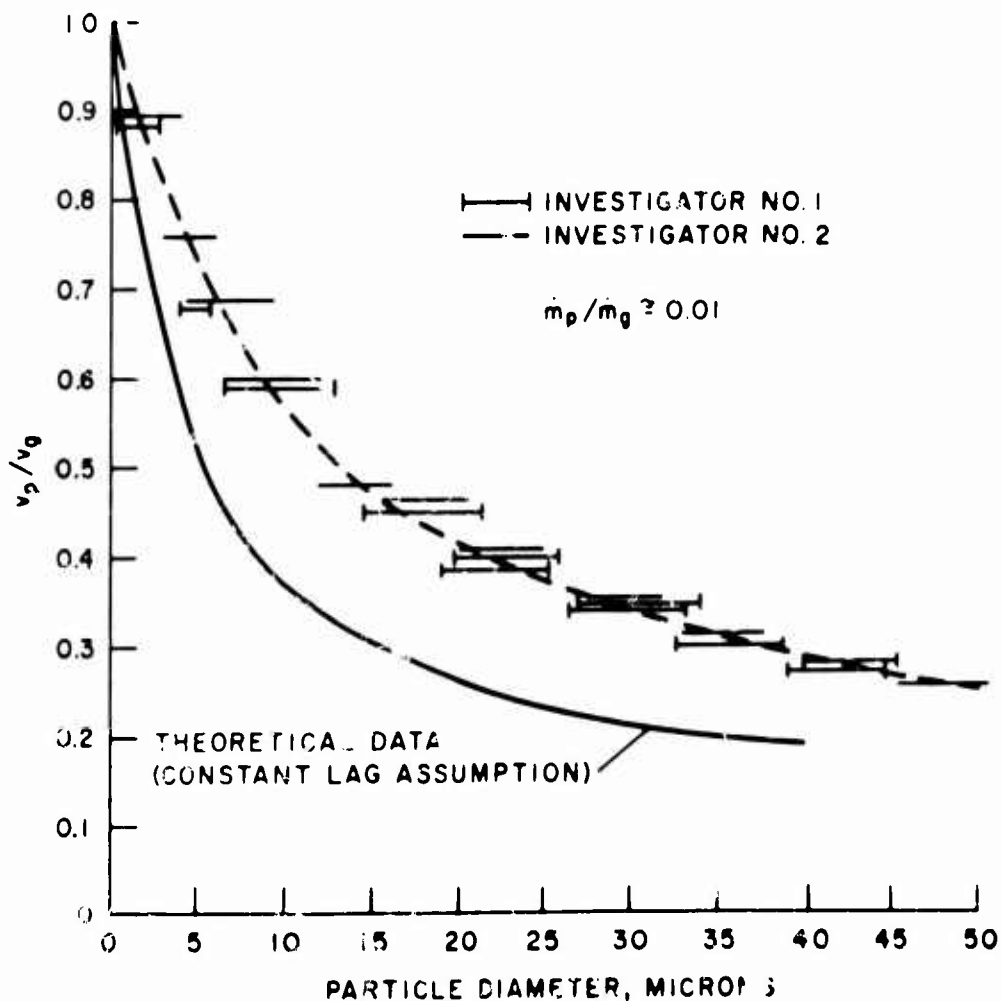


FIG. 24. Normalized Particle Velocity as a Function of Particle Size Using a Helium Carrier Gas Moving at 2,900 ft/sec.

For comparison purposes, theoretical data was also plotted on the graph. The theoretical values were calculated using one-dimensional particle flow equations and assuming a constant particle-to-gas velocity ratio (Ref. 8-9). The assumption simplifies the solution of the equations and the results of which agree quite well in the throat region with the generalized one-dimensional calculations.

The procedure given in Ref. 9 was used for the calculations. The pressure in the chamber was taken as 30.5 psia and the temperature 80°F. The throat diameter was 0.125 inch with a 16-inch nozzle curvature radius at the throat. It was assumed that the particle-to-gas mass flow fraction was negligible. At the suggestion of Dr. Crowe of United Technology Center, the constant in Eq. A-9, Ref. 9 was changed from .612 to 0.73. This was to account for the fact that gradients in the nozzle used in the experiment differed from those in the usual axisymmetric nozzle.

It can be seen in Fig. 24 that the trends of the two curves agree fairly well. However, the velocity lag is not as great as predicted by the theory. The results indicate that a further extension and refinement of the work reported here would be desirable. A comparison of the data with two-dimensional theory would also be of interest.

#### CONCLUSIONS

A photographic technique was developed whereby it was possible to directly measure the velocity of particles as small as 2 to 3 $\mu$  traveling at velocities up to 2,600 ft/sec in a helium-gas stream. The fractional standard deviation varied from 1.5 to 3.2% depending on the velocity of the particle. It is felt that, by optimization of the technique, it should be possible to extend the measurements to higher particle velocities and possible hot-flow conditions using relatively nonluminous gases.

Individual particle velocities were measured for aluminum powder fractions in a 2,900 ft/sec helium-gas stream. Particle velocities and sizes were correlated and the results compared with theoretical data. Although the trends of the experimental and theoretical data correlate fairly well, it appears that particle lag is not as great as predicted by the theoretical calculations.

## Appendix A

SURVEY OF PHOTOGRAPHIC METHODS FOR THE DIRECT  
MEASUREMENT OF PARTICLE VELOCITIES

After considering the possible techniques which might be used to measure the velocity of individual particles traveling at the high velocities encountered in rocket exhausts, it was concluded that photographic approaches hold the most promise for solving the very difficult problem. A number of photographic techniques have been studied to determine if any could meet the requirements for such a task.

Studies have shown that the particles of interest lie in the range below  $10\mu$  (Ref. 10) and have an upper velocity of about 5,000 ft/sec. Limitations in lighting resulting from wavelength considerations set the lower limit at around  $1\mu$ . Thus, any system to be of interest should have potential for measuring the velocity of 1 to  $10\mu$  particles traveling at speeds up to 5,000 ft/sec.

Initial experimental conditions called for a system capable of measuring particle velocities under cold-gas conditions. However, the possibility of future tests in which measurement would be taken in an actual rocket exhaust dictated that techniques also be examined for use in hot-gas situations.

The techniques considered can be divided into two basic classes: (1) those in which the particles are backlighted, and (2) those in which they are frontlighted. In the first case the particle is silhouetted against a luminous background. This results in a photograph in which the entire background is exposed, with the exception of the particle image or shadow. In the second case the particle is emitting light (either through reflection or self-luminescence) against a dark background. Thus, only the particle image is exposed on the film.

When photographing a particle using backlighting, it is necessary to essentially stop the motion of the particle image on the film. If the particle image is allowed to move or streak across the film, it will travel into an area already exposed by the background light and, in turn, the spot of unexposed film initially in the shadow of the particle will become exposed. In this way the trace is easily washed out. Through frontlighting it is possible and usually desirable to allow the particle image to streak across the film, since light from the particle and not from the background is the agent for exposing the film.

From the foregoing discussion, it can be seen that a much faster shutter will be needed for the backlighting approach. To stop a  $1\mu$  particle traveling at 5,000 ft/sec within a distance of one particle diameter, as required with backlighting, takes an exposure time on the order of 1 nanosecond ( $10^{-9}$  sec). With direct lighting techniques

exposure times on the order of 1 microsecond ( $10^{-6}$  sec) or longer are sufficient.

Because of the difficulty inherent in distinguishing a dot-type image as obtained with backlighting as compared with the streak-type image usually found with frontlighting techniques, a higher magnification will be necessary when the backlighting approach is used. It is much easier to locate a streak that is  $10\mu$  wide and 1 inch long on a piece of film than it is to identify a dot  $10\mu$  in diameter among the film grains. For frontlighting techniques it appears that magnifications in the range from 5X to 10X are sufficient. For use with backlighting, a magnification of 25X would most likely be needed to obtain good results. Additionally, if the light is overly bright, halation will occur; with frontlighting, the particle image will appear larger. With backlighting, however, the halation tends to wash out the image and decrease the effective particle size.

In both cases, however, delivering sufficient light to the film is one, if not the most important, consideration. For the backlit approach where an extremely fast shutter is used, and for frontlighting where the particle image is streaking across the film at a high velocity, the effective exposure time for the image at any spot on the film will be on the order of several nanoseconds. Thus, to deliver sufficient light to the film with such short exposure times, a fast optics system, very sensitive film, and an extremely bright light source are required.

The light flux delivered to the camera is much greater with backlighting than with frontlighting. In the first case the light source itself is being photographed, whereas in the second case the light is being reflected from the particle surface or generated from the relatively weak emittance of a hot particle. (Consider the difference in exposure time needed to photograph an object silhouetted against the sun compared to that needed to photograph the same object illuminated by the sun rays). However, this light advantage is partially offset by the need for higher magnification when using backlighting, since the light intensity to the film decreases in general as a function of the square of the magnification. For frontlighting, in particular, sufficient lighting appears to be quite difficult.

#### BACKLIGHTING TECHNIQUES: MULTIPLE EXPOSURES

Because of the spot-type image necessary with backlighting, a multiple exposure technique would be necessary to measure particle velocity. Through multiple exposures the particle's motion history could be recorded as a series of dots. Knowing the distance the particle traveled between exposures (obtained from the magnification of the camera optic system and the distance between image dots) and the time interval between exposures, the velocity can be calculated. Ideally,

multiple exposures would be made on one film, giving a series of "dots" across a single picture. As discussed earlier, repeated exposures on one film would result in an image washout because of the luminous background. It would be necessary to use some system in which two or more separate photographs could be obtained. To accurately determine velocity it would be necessary to arrange the cameras so that it would be known exactly how the two pictures were related spatially. This could be done by either making sure the cameras were photographing the identical area, such as could be accomplished with a beam-splitting arrangement (Fig. 25), or through the use of some background reference system. Ideally, the resulting pictures would appear as in Fig. 26.

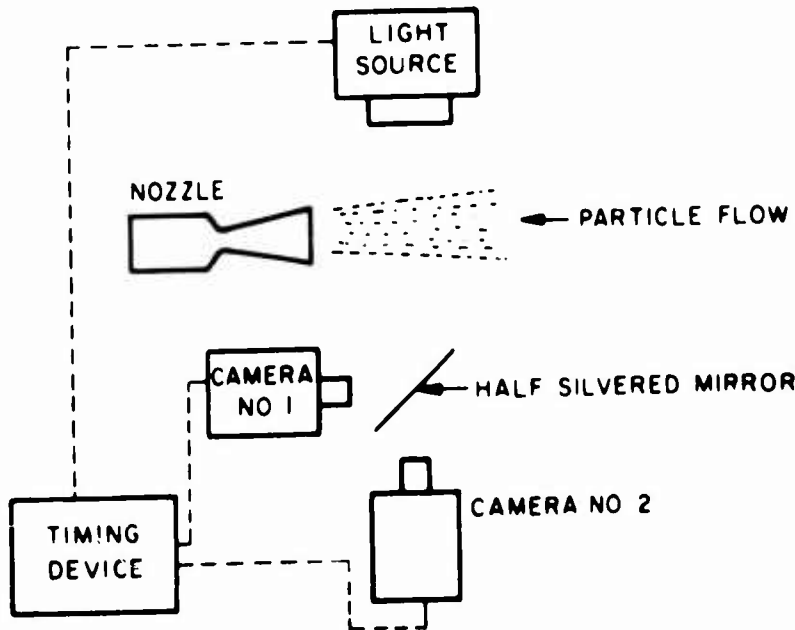


FIG. 25. Schematic Drawing of Multiple Image Backlighting Setup.

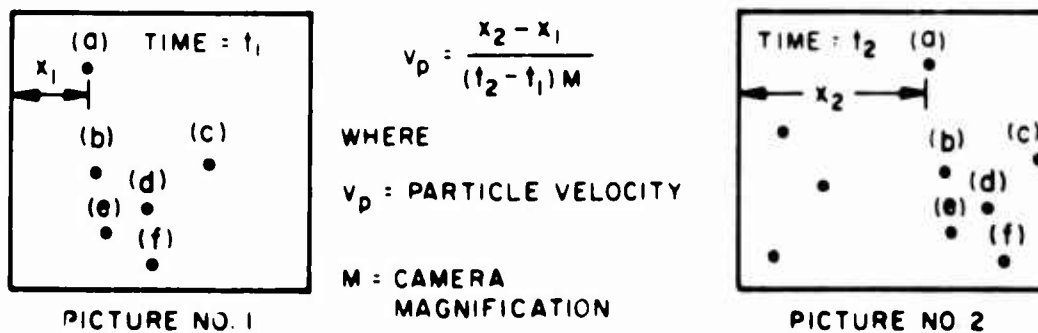


FIG. 26. Idealized Pictures Obtained With Multiple Image Backlighting Technique (Fig. 25).



Only one shutter was found that approached the required 1-nanosecond exposure time and had the necessary resolution. This was the electro-optic-type Kerr-cell shutter with a minimum exposure time of 5 nanoseconds. It is possible that photographs of some of the particles in the larger sizes ( $5\mu$  and over) could be stopped at these exposures.

Additional problems would exist in identifying any given particle from one picture to another unless the particle density in the field was quite low. Because of the very shallow depth of field resulting from the high magnification, particles might appear in one photograph and not in the second, further confusing the assessment.

#### FRONTLIGHTING TECHNIQUES

If the serious problem of obtaining sufficient illumination can be overcome, frontlighting appears to be more versatile than the backlighting approach. The possibility of streaking the image opens a number of avenues not possible with a spot-type image.

#### Single Streak Imaging

One of the most straightforward approaches to the problem of determining particle velocities would be to take a precision "time exposure" of the stream allowing each particle to produce a streak whose length is proportional to its velocity (Fig. 27). Measuring the length of the streak on the photograph and knowing the exact exposure duration and camera-lens magnification, it would be possible to determine the desired velocity. Of course, the "time exposure" would be very short, about 2 to 5 microseconds.

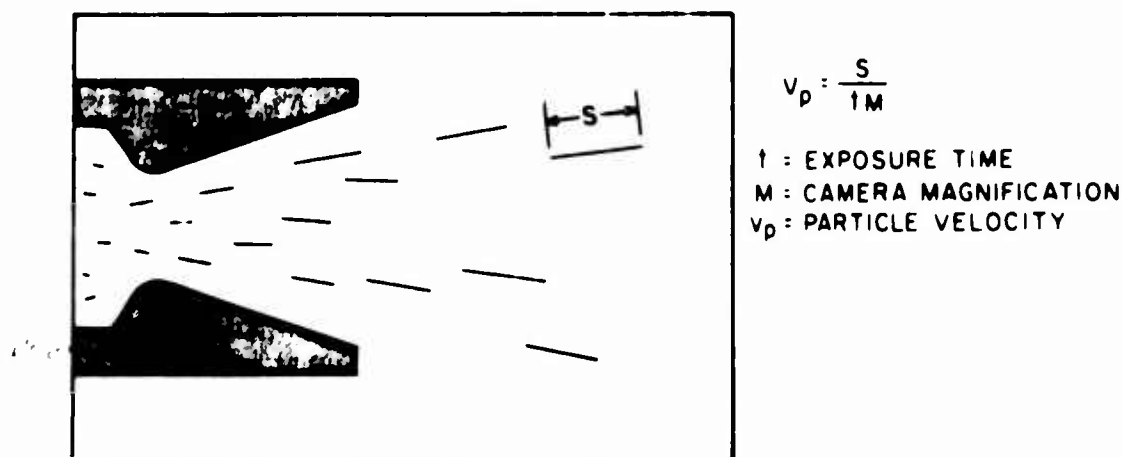


FIG. 27. Idealized Picture From Single Streak Technique.

The primary difficulty with this technique arises in determining the exposure time with sufficient accuracy. It is necessary to either have square wave shuttering (extremely short opening and closing times) or to know at what time in the shuttering operation sufficient light has been transmitted to start exposing the film, and to know when sufficient light has been cut off to terminate the exposure.

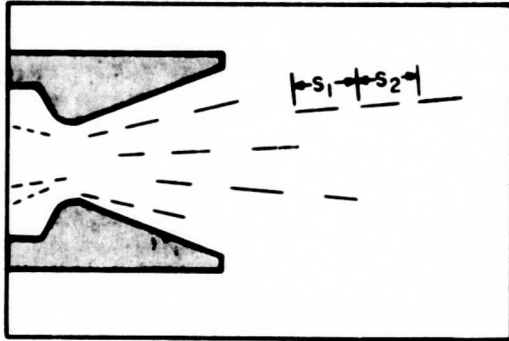
Exposures of the required duration can be obtained through the use of some type of shuttering device attached to the camera or through control of the duration of the illuminating light pulse. Two types of camera shuttering devices were considered: (1) electro-optical shutters (Kerr cells), and (2) image converter shutters. The electro-optic-type shutter appears to hold the most promise. Rise and decay times of about 1 nanosecond result in a nearly square wave shuttering for pulse lengths in the 2 to 5 microsecond range. Light transmission is relatively poor; at best about 39% of the entering light is transmitted. This, of course, adds to the already serious illumination problem. Some image converters also have good square wave characteristics, but at present the definition is quite poor for particle pictures because of the grainy structure of the converter-tube phosphor. The relatively small photo size is also a drawback.

Sparks, exploding wires, flash tubes, and explosive rare-gas light bombs can be used to produce short light pulses of about the correct duration. With the exception of the explosive rare-gas light bombs described in some detail in the text and Appendix B, it is questionable whether sufficient light could be derived from these sources over a reasonable field of view. Additionally, all depart significantly from the desired rapid decay times needed, but work has been done at NOTS which indicates that rapid decay times may be possible with the light bomb (Ref. 6).

If the tailoff or long decay times can be controlled, the use of light-shuttering would provide a relatively inexpensive means for photographing either a cold-gas flow or a relatively nonluminous hot flow. By conducting the experiment in a dark room, the camera shutter would be used only for capping purposes and a simple press camera could be used. If the flow were somewhat luminous or if it were necessary to run in a luminous environment, a capping shutter would have to be used that was sufficiently fast to reduce background lumination to a tolerable level.

#### Multiple Exposure Techniques

Multiple exposure techniques, discussed previously under backlighting approaches, are also amenable to frontlighting. By exposing the film two or more times, a series of streaks can be produced (Fig. 28). From the spacing of the streaks it is possible to determine the velocity of the parent particles. If three or more exposures are taken, acceleration can also be obtained from the difference in particle spacings.



$$v_p = \frac{S}{tM}$$

$v_p$  = PARTICLE VELOCITY

$t$  = TIME BETWEEN EXPOSURES

$M$  = MAGNIFICATION

FIG. 28. Idealized Picture From Multiple Streak Technique Frontlighted.

Since there is no image washout when photographing a reasonably sparse particle field with frontlight, the series of streaks may be recorded on one piece of film. This should provide a more accurate velocity measurement than that obtained with backlighting techniques in which it is necessary to record each exposure on a different piece of film. Additionally, the streaks obtained with frontlighting, unlike the dots recorded in backlighting, indicate the direction of particle travel. This is very useful when determining which traces belong to a single parent particle. As discussed previously, the velocity of the particle is calculated from the distance between streaks on the film, the time interval between exposures, and the camera magnification.

Because of the relatively short time between exposures (about 2 to 5 microseconds), it is likely that light-shuttering would be necessary if the series of streaks were to be captured on one piece of film. No camera shutter was found capable of recycling this fast. However, by using multiple light sources of short duration (about 1 microsecond) and high intensity activated at precise intervals, the desired results are possible. With light-shuttering it will be necessary to work with a relatively nonluminous flow under either darkened conditions or with a fast capping shutter to reduce background light to a tolerable level.

The explosive rare-gas light bombs are especially amenable to this multiple exposure technique. A variation of this approach was used in the cold flow experimentation reported here. Detailed discussion is provided in Appendix B and the section titled Lumination.

Unlike the single streak approach, it is only necessary to have either the front or the back of the streaks sharp and well defined (half-square light pulse) since measurements are usually taken from identical points in each streak. A number of different type light sources having sharp rise times but poor tailoff characteristics might find application.

### Streak Camera Technique

It may be possible to adopt standard streak camera techniques for the measurement of particle velocities. With this type camera the film is effectively moved through the image frame at a known rate; or where high writing speeds are necessary, the image may be swept across a stationary strip of film by the use of a rotating mirror or prism. Knowing the effective speed of the image sweep, it is possible to determine position or displacement as a function of time. Thus, a stationary point of light would appear as a line parallel to the direction of film travel (time axis). If the light were moving at right angles to the film motion (displacement axis), a continuous record of position versus time would be recorded in the form of a sloping line. The slope (first derivative) of the resulting trace would represent the velocity, while the second derivative or change in slope of the line would provide a value for acceleration. A more detailed description of the streak camera can be found in most texts on high speed photography (Ref. 11-12).

A simplified schematic sketch illustrating how streak camera techniques could be used to measure particle velocity is given in Fig. 29. In reality it would be necessary to use a rotating mirror-type camera in order to obtain the necessary writing speeds (about 50,000 ft/sec at a 10-to-1 magnification). For best measurements, the writing speeds should approximate the particle image speeds. The slit shown is used to narrow the field of view. This is necessary in order to eliminate the confusion resulting from a number of streaks in different portions of the nozzles, (at different times), tracing through the same point on the film.

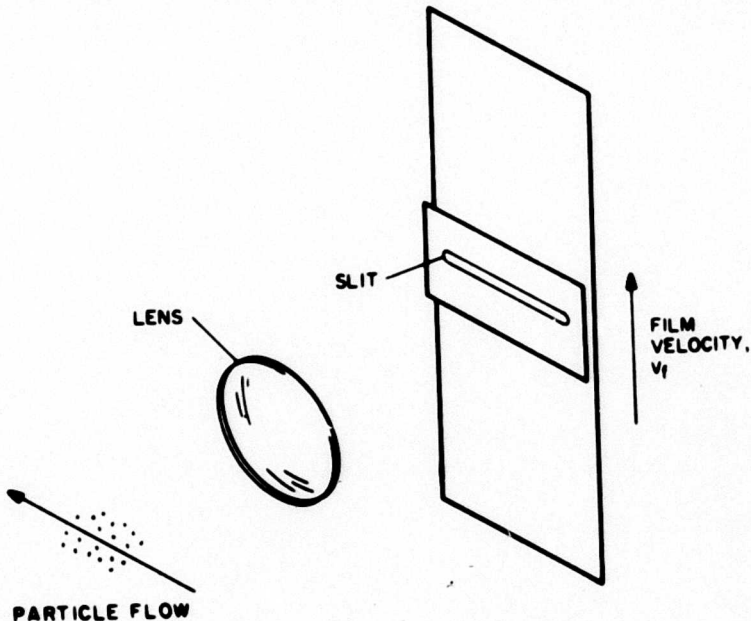


FIG. 29. Schematic Diagram of Streak Camera Setup for Photographing Particle Flows.

Figure 30 shows how an idealized record might appear. Knowing the effective film velocity (sweep speed),  $v_f$ ; the camera magnification,  $M$ ; and the angle of the streak with respect to the displacement axis,  $\alpha$ ; the particle velocity can be calculated from

$$v_p = \frac{v_f}{M \tan \alpha}$$

Using graphical methods, acceleration can also be determined.

The streak camera technique appears quite promising. The light intensity will need to be greater, however, because of the velocity component of the film or image sweep (Fig. 30). However, the shape of the light pulse will not be critical as in some of the proposed techniques. The main benefit is derived from the continuous record of particle velocity and the capability for measuring acceleration. The camera, however, is rather large and expensive.

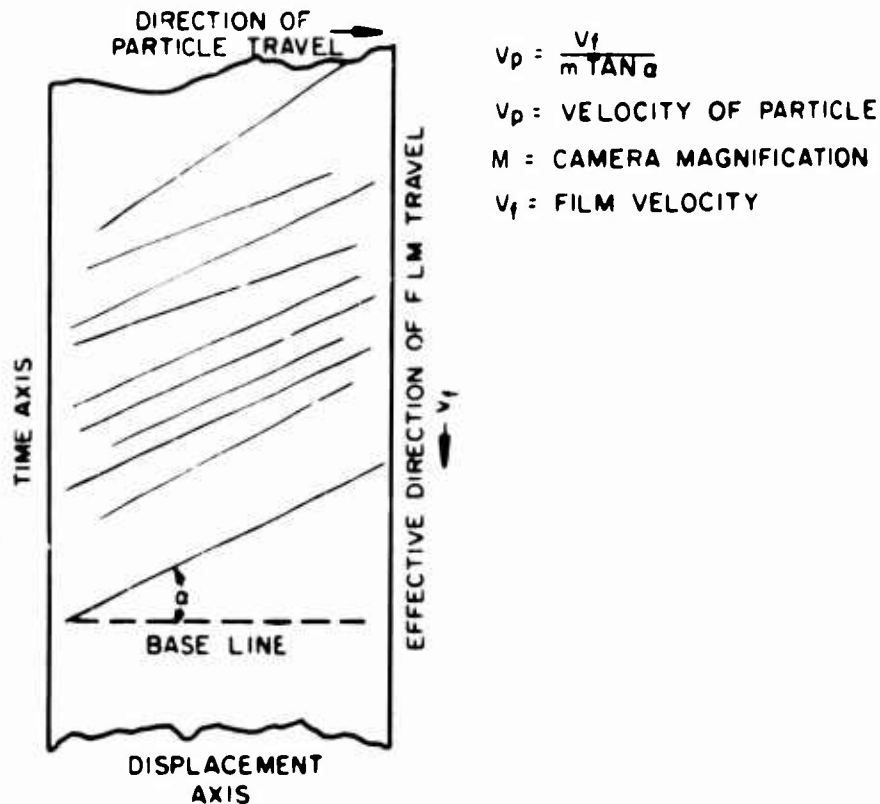


FIG. 30. Idealized Picture Obtained With Streak Camera Technique.

Synchroballistic Technique

The streak camera is used in a different manner in the synchroballistic technique. Here the camera is rotated 90 degrees so that the film

or the speed of the image sweep to exactly counter the movement of the particle image, it is possible to stop the image at one spot on the film. Knowing the sweep speed and the optics of the camera system, the velocity of the particles traveling at that particular speed (critical velocity) can be determined. If the particles are traveling faster or slower than the critical speed, a streak will result whose length is proportional to the difference between the critical speed and the particle speed. This then, breaks down to a variation of the single streak technique and it becomes necessary to know the light duration and streak lengths to calculate the velocity difference, and in turn, the true velocity. Carlson at Aeronutronic used this technique with some success to measure the velocity of particles traveling at high velocity. A description of this technique and the results can be found in Ref. 2.

The primary benefit of the synchroballistic technique lies in the increased effective exposure times which reduces the lighting problems. However, unless the light intensity is maintained at a high level, the range of particle velocities which can be picked up by streaking becomes limited. In addition, it appears that in those cases where streaks result, it would be most difficult to determine if they represent particles traveling faster or slower than the critical velocity. As with a number of the other techniques, it is not possible to determine accelerations with the synchroballistic approach.

Appendix B

EXPLOSIVE RARE-GAS LIGHT BOMB

The construction and design of the light bomb incorporates various principles from such fields as optics, gas dynamics, and impulsive loading. The light bomb required a trade-off between the light output and the impulsive strength of the materials. In most cases systems incorporating impulsive loading are too time-consuming to optimize because they require empirical data. The time allocated for the basic construction of the light bomb was short, and the resulting system was not optimized.

LIGHT-BOMB HOUSING

The light-bomb housing consists of a cylinder, front and back plates, baffles, and a cradle base (Fig. 31). The cylinder is 8 inches long and is constructed from a 5-inch OD mild steel stock with 1/2-inch walls. The mild steel end plates have an outer edge thickness of 3/8 inch which is increased to 1/2 inch at the inside diameter of the housing for ease in assembly and added bulging strength. The end plates are connected by six equally spaced 5/16 Allen head bolts 3/4 inch long. The front plate has a 2-inch diameter port. The rear of the housing has two symmetric 2-1/2 x 1-1/4 inch ports to allow the reaction products to escape. In front of these ports and on the inside, 1/2-inch thick circular segment baffles are welded to help restrict fragments from leaving the ports (Fig. 31). A cradle is bolted to the bottom of the housing which allows easy attachment to a tripod (Fig. 7) for support and positioning.

INNER SYSTEM

The inner system (the heart of the light source) is shown with the lenses and the front plate in Fig. 2 and 32. This area of the light source required the greatest amount of design and testing and was destroyed during each test. For purposes of explanation, the inner system of the light bomb will be divided into three subsystems: the buffer, the light pulse, and the explosive.

Buffer Subsystem

The primary purpose of the plastic buffer discs was to protect the condensing lenses while at the same time allowing the large solid angle of light to pass through the front end plate. The buffer region, therefore, has to be as thin as possible to conserve the solid angle, but still be sufficiently thick to prevent scabbing of the front buffer surface which might break the lenses.

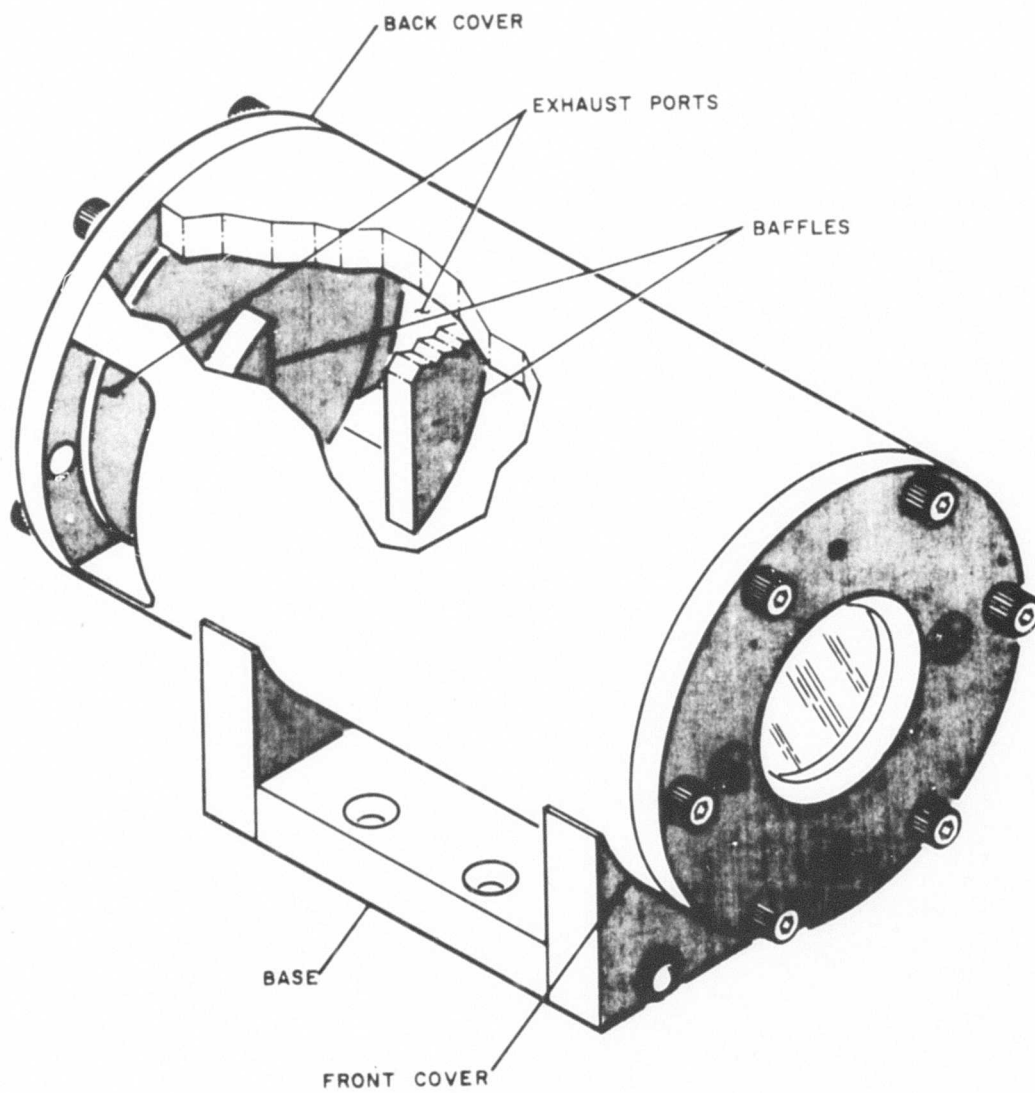


FIG. 31. Light-Bomb Housing.



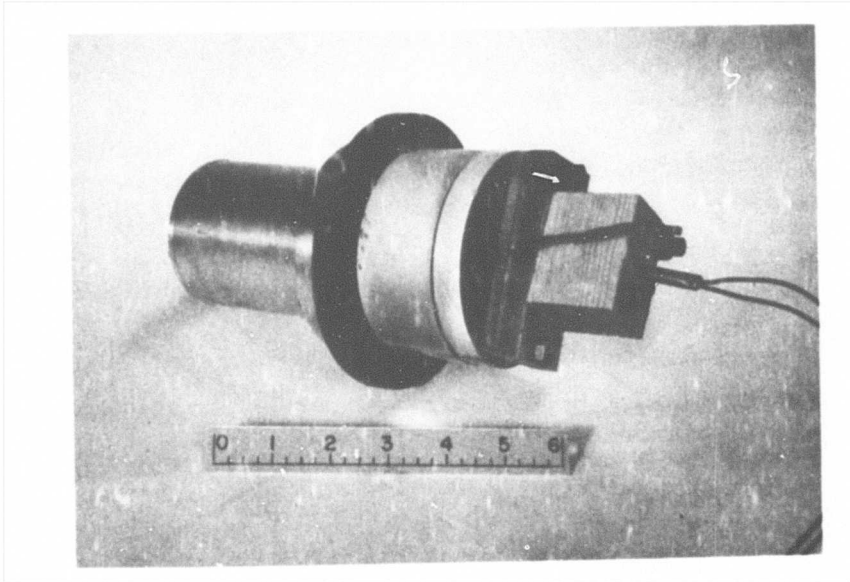


FIG. 32. Assembled Inner Light Bomb System.

The buffer subsystem was composed of two plexiglass discs  $1/2$  and  $1-1/2$  inches thick with a common diameter of  $3-3/4$  inches. The two pieces of plexiglass were separated by a narrow air gap. The purpose of the air gap was to form an impedance mismatch and thereby help to attenuate the stress wave entering the second piece of plexiglass. As a result of the air gap, part of the stress wave was reflected back into the first piece of plexiglass which was completely shattered. The second piece of plexiglass showed a few fractures but did not scab. Tests performed without the air gap resulted in scabbing of the second plexiglass buffer.

#### Light Pulse Subsystem

The light pulse subsystem is composed of two rectangular plates  $1-1/2$  by  $3-1/2$  inches with  $1/2$ -inch holes in the centers as shown in Fig. 2. Air is contained in the first  $1/4$ -inch plate and the rare gas in the second  $1/2$ -inch plate. The rare gas was enclosed in the  $1/2$ -inch diameter gas gap by placing transparent Scotch tape on both sides of the aluminum plate, and was introduced into the gas gap by either continuously flushing the gas or by encapsulation after first evacuating the space. Both argon and krypton were tested and the results were inconclusive as to which rare gas yielded the higher light intensity. The flushing technique was used with argon gas which was easy to obtain and much less costly. This was accomplished by flowing argon into the gap through a  $1/8$ -inch copper tube which connected into the gap. A second  $1/8$ -inch hole to the outside allowed the gas to exhaust. The technique

used to encapsulate the krypton gas incorporated a plate similar to the one used with the flush technique, but without the exhaust port. Using hand valves, a vacuum gage, and the usual Scotch tape on both sides of the plate, the gas gap was evacuated, after which argon gas was bled into the gap. This procedure was repeated; after evacuating the gap a third time, krypton was bled into the gap. The inlet line was then sealed.

The air gap was constructed from a 1/4-inch thick plexiglass plate. Although the use of plexiglass was a matter of availability, the thickness of the air gap was dictated by empirical results. The 1/4-inch air gap was used since it allowed enough distance for the light intensity produced in the rare gas to decrease below the sensitivity of the film, and also resulted in a total light pulse of the required duration of about 3 microseconds.

The basic operation of the light pulse subsystem can be stated as follows: A shock wave produced by the detonated explosive enters the rare gas, which in turn is excited to a high energy level, and emits an intense light. As the wave enters the air gap, the intensity of the light drops off radically since air required a much higher energy level to emit an intense light. However, as the shock wave (which has an average velocity of 20,000 ft/sec) impacts the plexiglass, the air at the interface is raised to an extremely high energy level and re-emits an intense light upon returning to its ground state. Figure 33 graphically shows the operation of the light pulse subsystem.

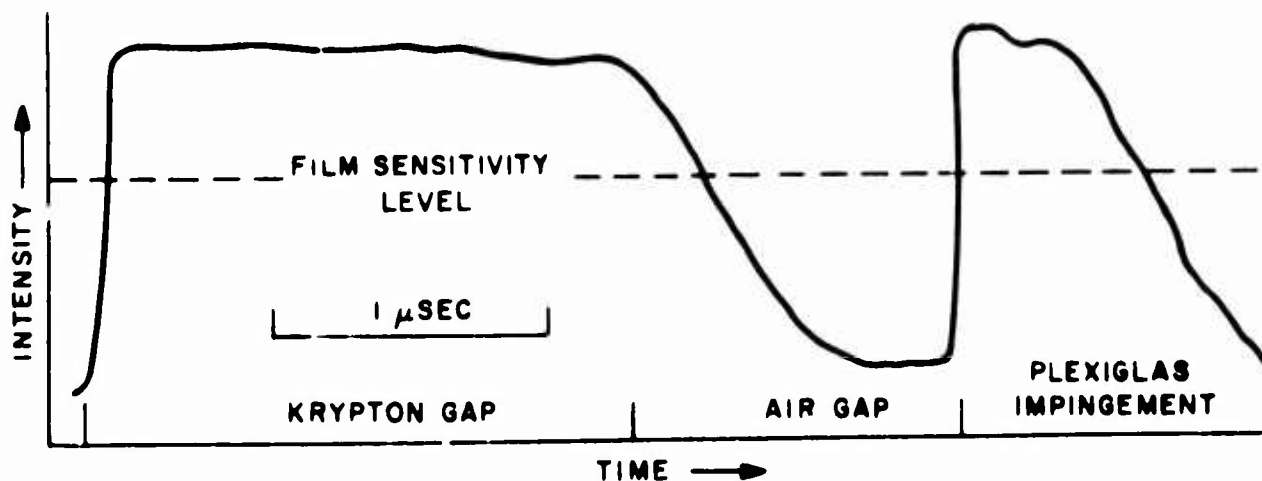


FIG. 33. Dual Streak Light Pulse Pattern.

#### Explosive Subsystem

The explosive subsystem is composed of two 1/2 x 1/2-inch tetryl pellets, an electric detonator, and a wood block used for positioning the explosives and detonator (Fig. 2). The wood block was used since

wood fragments are relatively safe compared to metallic or brittle materials. The wood positioning block measures 1-1/2 x 2 x 1-1/2 inches with a 1/2-inch diameter hole drilled in the center 1-1/8 inches deep followed by a 9/32-inch diameter hole on the axis for the detonator. The two tetryl pellets were placed in the hole with care taken, first, not to break the pellets which are quite brittle and, second, to maintain the face of the explosive in the same plane as the face of the wooden block. The explosive subsystem was bolted to the gas gap plate as shown in Fig. 2.

The use of two tetryl pellets in tandem was required to produce a nearly true plane detonation wave at the explosive gas interface. A small explosive plane-wave generator could be used instead of the two tetryl pellets. The generators produce a more nearly true plane wave than the pellets, but the degree of difference did not warrant its use because of the cost and difficulty involved.

The figures are self-explanatory as far as the interconnection of the various subsystems are concerned. However, the 1/2-inch diameter center axis should be carefully aligned so that there is nothing to impede the shock wave.

#### LENS SYSTEM

The lens system is required to condense the solid angle of light emitted through the front cover of the light source down to the small field of view. This maintains high intensity light on the particles in the field of view.

The light-condensing lens system is shown in a cutaway drawing in Fig. 34 including the system construction and dimensions. The two most conspicuous features in the design of the lens system are the use of two condensing lenses and the mounting of the lenses to protect them from impulsive loads.

Two lenses instead of one are used in the system because of the resulting greater flexibility. Lens 1 is positioned at approximately one focal length from the light source so that the light is turned essentially parallel to the axis. The second lens can be placed at a reasonable distance away (Fig. 4) which is beneficial due to the limited space available for both the camera and the light bomb. By varying the focal length of lens 2, one can vary the image size to which the light is condensed. Both lenses are plano-convex and need not be of high quality, since precise focusing of the light is not required.

As noted in Fig. 34, the lenses are not rigidly mounted. They are held between rubber O-rings allowing them to move under stress. One test was run in which the lens system was rigidly mounted. This resulted in fragmentation of the lenses, primarily on the edges where they were

mounted. The lens system is bolted to the front cover of the light bomb which is separated by a rubber O-ring buffer. This buffer helps to impede the stress wave from being transmitted to the lens housing.

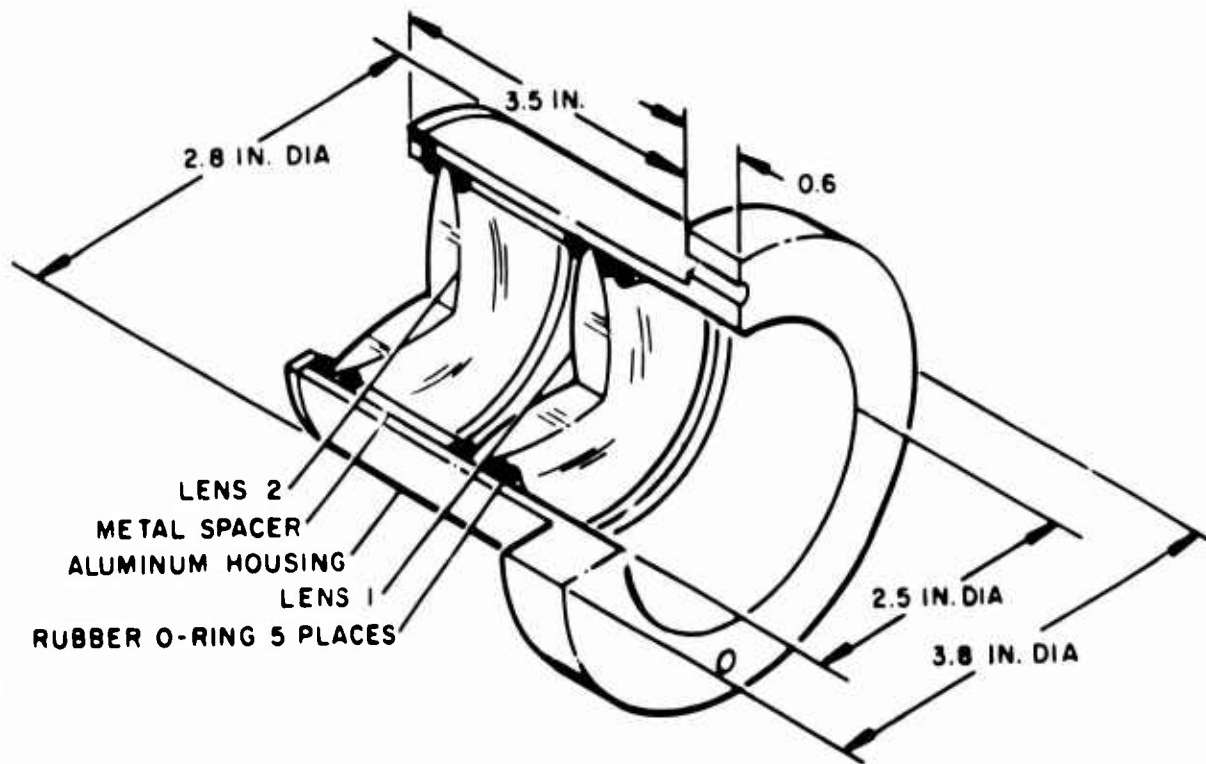


FIG. 34. Light Condensing Lens System.

REFERENCES

1. Kliegel, J. R., and G. R. Nickerson. "Flow of Gas-Particle Mixtures in Axially Symmetric Nozzles," ARS Preprint 1713-61 (1951).
2. Aeronutronic Division, Philco Corporation. An Investigation of Recombination and Particle Lag Effects in Rocket Nozzles (U), by W. Kuby, and others. Newport Beach, Calif., Aeronutronic, 15 December 1963. (Publication No. C-2378), CONFIDENTIAL.
3. Neblette, C. B. Photography—Its Principles and Practices, 4th ed. New York, Van Nostrand, 1927.
4. Presman, Zev. "High Intensity Explosive Light Sources." Proceedings, Fifth International Congress on High Speed Photography, 1962.
5. U. S. Naval Ordnance Test Station. A Portable, Blast-Contained, Explosive Light Source for High-Speed Shadowgraphs, by Rolland Gallup. China Lake, Calif., NOTS, 21 February 1962. (NAVWEPS REPORT 7880, NOTS TP 2862).
6. Plauson, R. A., and H. Dean Mallory. "Extinction of Gas-Shock Luminosity Against Transparent Surfaces," J APPL PHYS, March 1964, (Vol. 35, No. 3, Part 1), p. 502.
7. Berg, U., and P. A. Persson. "Multiple Flash-Gap Technique for Measuring Shock Wave Velocities", NATURE, 5 January 1963, Vol. 197, pp. 65-66.
8. Space Technology Laboratories. One-Dimensional Flow of a Gas Particle System, by J. R. Kliegel. Los Angeles, Calif., Space Technology Laboratories, 1959, (TR-59-0000-00746).
9. United Technology Center. Dynamics of Two-Phase Flow, Twelfth Quarterly Technical Progress Report for Period 1 February 1964 through April 1964, by C. T. Crowe, and others. Sunnyvale, Calif., United Technology Center, 28 May 1964. (UTC 2005-QT12).
10. Jet Propulsion Laboratory. An Experimental Investigation of a Gas-Particle System, by Robert Sehgal. Pasadena, Calif., Jet Propulsion Laboratories, March, 1962 (Technical Report No. 32-238).
11. Hyzer, William G. Engineering and Scientific High-Speed Photography. New York, Macmillan, 1962.
12. Chesterma, W. Deryck. The Photographic Study of Rapid Events. London, Oxford, 1951.